859

NUCLEAR FUEL TRAJECTORY ANALYSIS

FUEL TRAJECTORY ANALYSIS OF ADVANCED NUCLEAR ENERGY FUEL CYCLES AND SYSTEMS

by

JAMES KEVIN PRESLEY, B.Sc.

A Thesis
Submitted to the School of Graduate Studies
In Partial Fulfilment of the Requirements
for the Degree
Master of Engineering

McMaster University

1980

MASTER OF ENGINEERING (1980)
Engineering Physics

McMASTER UNIVERSITY
Hamilton, Ontario

TITLE: Fuel Trajectory Analysis of Advanced Nuclear Energy Fuel Cycles and Systems

Part A

AUTHOR: JAMES KEVIN PRESLEY, B.Sc. (University of Waterloo)

SUPERVISOR: Dr. A.A. Harms

NUMBER OF PAGES: viii, 58

ABSTRACT

The unique features of the Interrupted Thorium Cycle owing to Pa-233 have been examined including possible implications for practical implementation of the cycle. Generalized trajectories for the fuel inventories of fusion-fission symbionts are derived through a comprehensive parametric analysis. The resultant formulations are then applied to a specific example. It is concluded that this formulation and analysis leads to more exact fissile and fusile fuel characterizations than suggested by conventional procedures.

ACKNOWLEDGEMENTS

I would like to thank Dr. A.A. Harms for his untiring guidance throughout all stages of this work. Thanks are also due to my wife Janet for helping keep up my morale at all times not to mention the typing of the first draft. I would also like to thank Ms. Janet Delsey for typing the final draft.

TABLE OF CONTENTS

LIST OF TABLES

LIST OF FIGURES

CHAPTER 1

INTRODUCTION

Concerns regarding the supply of U-235 as a fuel for fission reactors have resulted in extensive efforts to develop breeder reactors for the production of fissile fuels. The use of neutrons produced by a fusion reaction for the purposes of breeding fuel has been the subject of research for some time now.[1] This arrangement consisting of a fusion reactor surrounded by a breeding blanket to produce/burn fissile fuel is generally referred to as a fission-fusion reactor.

In the consideration of such a system it is possible to envisage a number of variations on the fission-fusion theme. At the most fundamental level the different variants could utilize various fuels for the fusion reactor and/or the fissile/fertile material contained within the breeding blanket. Other possible systems could differ in the manner in which both the fusion and fission reactions are exploited for energy production, breeding, etc.

For fusion reactors some possible reactions are illustrated in Table 1.0-1. At present it appears, for various reasons, the most promising of these reactions for use in fusion power reactors will be the D-T reaction.

With respect to the fertile fuels to be used for fissile fuel breeding there are two possibilities, namely U-238 and Th-232. The fissile fuels produced from the former are the Pu-239 and U-233 respectively.

TABLE 1.0-1: Fusion reactions of interest for Fusion reactors.

Reactants	Products	Energy Released (MeV)
D,T	n,^{4}He	17.6
D,D	n,^{3}He	3.2
D,D	p,T	4.0
D,^{3}He	p,^{4}He	18.3

As previously mentioned it is also possible to vary the manner in which the fission or fusion reactors are deployed. One method, the "Hybrid", involves surrounding a fusion reactor with a fission reactor to utilize the fusion neutrons directly, for power production with breeding essentially assuming a secondary role. An alternate possible arrangement, the "Symbiont", has the reactors separated with appropriate connections for isotope transferral between them.

1.1 Research Area Defined

This research is involved with an analysis of fuel trajectories for some of the possible fission-fusion systems; in this context trajectory refers to a time dependent function which may be represented graphically. To this end the work is divided into two relatively distinct and separate sections. The first section examines the fuel trajectories for an analysis of a U-233 breeding system using fusion generated neutrons. The analysis actually utilizes generated fuel trajectories to aid in understanding specific physics aspects of a U-233 fuel breeding cycle. This cycle has been named the "Interrupted Thorium Cycle" because of time-related effects attributed to Pa-233 which is an intermediate product in the production of U-233 from Th-232. The second part of this research is concerned with fuel trajectories associated with a specific type of fusion-fission reactor, the Symbiont. In this case a parametric analysis has been done to develop general trajectories applicable to any Symbiont system.

1.2 The Need for the Present Research

Upon examination of previous work[1-10] dealing with fusion-fission systems it is apparent that there has been a distinct neglect of effects occurring in these systems caused by the presence of isotopes which have relatively short half-lives. The word short here refers to times in the range of approximately one month to ten years. In most, if not all, fission-fusion studies the 27.4 day half life of Pa-233 has been approximated as zero. As will become evident in Chapter 2 this time is non-negligible and accounts for some interesting effects in a U-233 breeding system. To date these effects have only been discussed in connection with Th-232 fuelled CANDU reactors.[11,12] The reason for the suppression of the Pa-233 half-life is because of the non-linearities introduced into relevant equations which make their solution far from trivial.

Another half-life which has been virtually ignored everywhere in connection with fusion-fission reactors is the 12.3 yr. half-life of T. As stated previously this is part of the fuel for a D-T fusion reactor. It will be seen in the third chapter that ignoring the decay of this isotope can lead to serious errors in the accounting of fuel for a Symbiont reactor.

1.3 Approach to be Followed

The intent of the second chapter is to bring to light interesting physical aspects of the use of Th-232 for breeding and power production. The purpose is not to design a reactor so to this end all spatial dependence of variables has been suppressed in relevant equations. As a

further simplification, calculations have been done using neutrons in only one energy group. Both approximations allow analytical results to be obtained which lend themselves to interpretation more readily than voluminous numerical results.

Chapter 3 utilizes a somewhat different approach from the preceding one. In the former a mathematical formalism employing a parametric description of a Symbiont has been developed. This formalism facilitates the calculation of fuel inventory trajectories given specific reactor parameters. This developed formalism is subsequently applied to a specific example of a Symbiont proposed by Blinkin and Novikov[13] for a critical examination of their results.

CHAPTER 2

THE INTERRUPTED THORIUM CYCLE

The use of U-233 as a fuel in thermal fission reactors has been recognized for some time as an effective means to extend the lifetime of nuclear fission power generation. For example, the writings of W.B. Lewis on this topic go as far back as the early days of the Chalk River Project.[14] This view still commands a good deal of time and effort in various research establishments throughout the world.[15,16] The attractiveness of U-233 as a fuel for thermal reactors is primarily due to two reasons. The first reason is that U-233 is produced by nuclear transmutation of Th-232 which is about three times as abundant as U-238 in the earth's crust. Secondly, the average number of neutrons released per fission, η, for U-233 undergoing fission at thermal energies is higher than the corresponding value for U-235. This fact makes U-233, neutronically, a more "economical" fuel for thermal reactors.

However, as previously stated, U-233 is not a naturally occurring isotope and must be produced by the nuclear transmutation of Th-232. The transmutation process is illustrated in Fig. 2.0-1. The preliminary reaction of interest occurs when Th-232 captures a neutron and is transformed to Th-233. This isotope, which is unstable, then undergoes β decay (half-life of 22 minutes) to become Pa-233, another unstable isotope. Pa-233 subsequently β decays (half-life of 27.4 days) into U-233. U-233 is α unstable with a half-life of 1.6×10^5 years. Also shown in the figure are associated possible reactions.

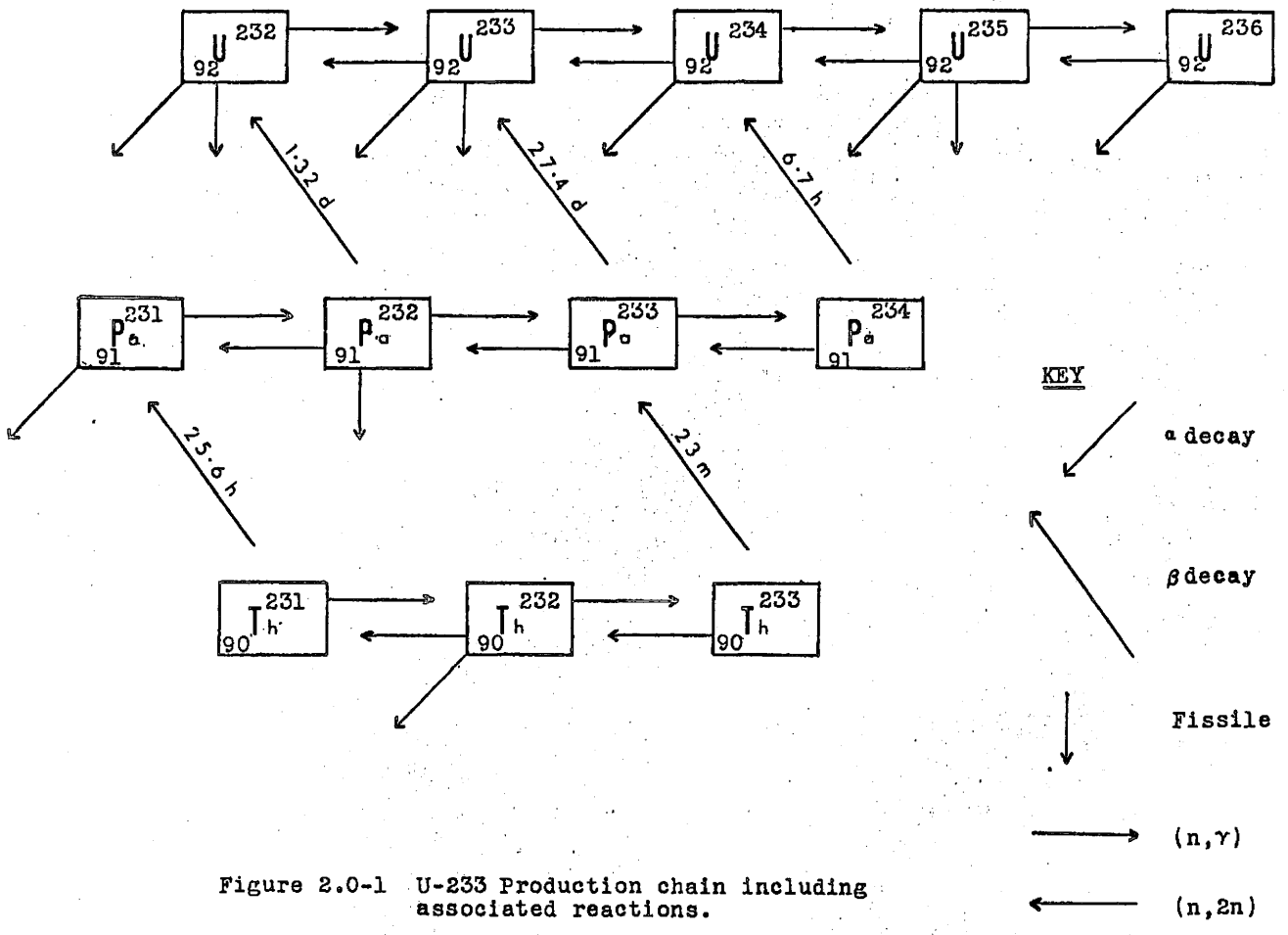

Figure 2.0-1 U-233 Production chain including associated reactions.

There have been a number of proposals put forth to utilize the forementioned chain for the production of U-233. Among the more prominent methods under study at present are electronuclear breeding,[17] and fusion breeding.[2,3] It appears however that most, if not all, studies have not addressed the implications arising from the non-negligible 27.4 day half-life of Pa-233. It is with respect to the temporal delay imposed by this half-life which the "Interrupted Thorium Cycle", hereafter to be represented by the acronym ITC, refers.

The concept put forth here is to irradiate a breeding material (say ThO_2) in a neutron flux for a specific time, then allow it to decay, removed from the neutron flux, at length until the desired concentrations of U-233 and Pa-233 have been attained. Subsequently, the fuel can be "burned" in a thermal fission reactor thus completing the cycle. This cycle consists of 3 phases; breed, decay, burn, respectively and can be repeated until materials considerations force the fuel to be "retired". Figure 2.0-2 illustrates the isotope trajectories for U-233 and Pa-233 during a typical cycle.

2.1 Effects of Pa-233 Half-Life on U-233 Breeding

The preliminary step in the analysis of the ITC is to understand the equations governing the isotope trajectories depicted in Fig. 2.0-2. If there are n isotopes under consideration in an isotope chain, then the concentration of any isotope, N_{ij}* is determined from a set of n differential equations;

---

* The standard convention is used here, i being the last digit in the atomic number, j the last digit in the mass number.

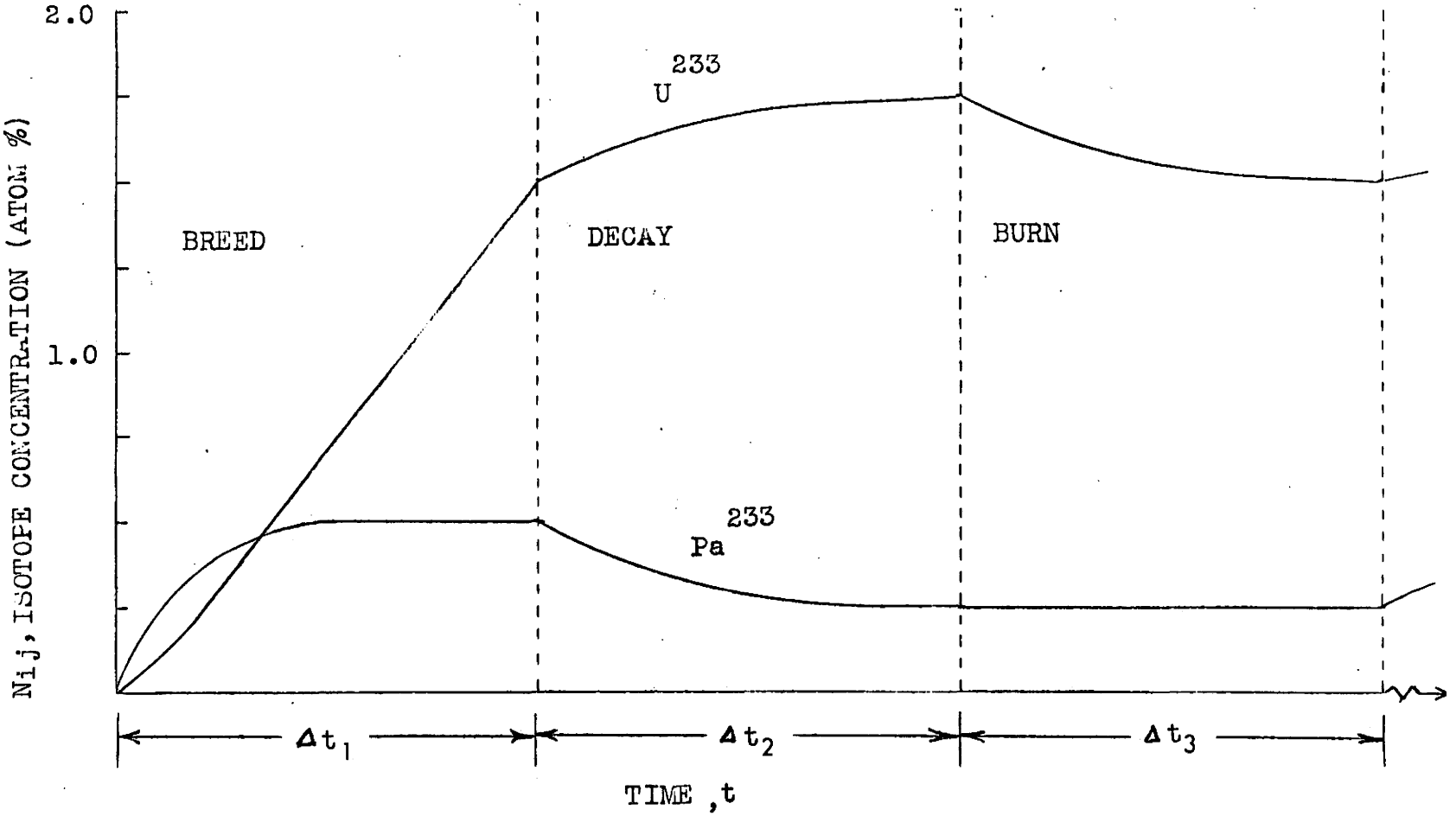

Figure 2.0-2 Typical isotope trajectories for the Interrupted Thorium Cycle.

$$\frac{dN_{ij}}{dt} = P_{ij} - R_{ij} \tag{2.1.1}$$

With P_{ij},R_{ij} being the isotope's production rate and destruction rate respectively given by;

$$P_{ij} = \sigma^{c}_{in-1}\ \Phi\ N_{ij-1} + \lambda_{i-1j}\ N_{i-1j} \tag{2.1.2}$$

$$R_{ij} = \sigma^{a}_{ij}\ \Phi\ N_{ij} + \lambda_{ij}\ N_{ij} \tag{2.1.3}$$

with

$$\sigma\Phi = \int_{0}^{\infty} \sigma(E)\Phi(E)dE \tag{2.1.4}$$

$$= \sigma(E_0)\Phi(E_0) \int_{E_2}^{E_1} dE \tag{2.1.5}$$

where

$$0 \leq E_1 \leq E_0 \leq E_2 \leq \infty$$

The equivalence of equations (2.1.4) and (2.1.5) is made possible by the integral mean value theorom. As a rule, σ, the reaction cross-section, and Φ, the integrated neutron flux, will be phase and time dependent. The emphasis here is on analytical and conceptual clarity so to this end accuracy will be sacrificed by assuming time independence of σ and Φ.

As another simplification, spatial dependence of all variables has been ignored. The reason for this approximation being that the specification of a breeding blanket and fission reactor is beyond the scope of this work. Notwithstanding, the use of the above approximations allow an analysis of some of the physics aspects of the ITC.

A convenient value of E_o for use in Eq. (2.1.5) would be the neutron energy for which the breeding efficiency of Th-232 is the highest. The effects of neutrons at this energy would depict the preferred energy range effects while also yielding insight into ITC physics. Figure 2.1-1 elucidates the energy value in question by illustrating the ratio of Th-232 capture cross-section to Th-232 absorption cross-section as a function of incident neutron energy. This ratio is a good indication of neutron breeding efficiency in a fusion breeding blanket because it is essentially the ratio of the probability of a breeding absorption to the probability of any absorption reaction. Examination of Fig. 2.1-1 shows a fairly broad flat peak in the range of about 10 to 50 keV. Consequently, data used in this study was that applicable to 30 keV neutrons.

It is possible, after generating the analytic expressions for the isotopic trajectories to utilize them in conjunction with appropriate boundary ocnditions to educe understanding of the underlying physics in the ITC. The boundary conditions referred to are those applicable at the temporal boundaries between each of the three phases of a cycle.

During the "burn" phase there is an equilibrium buildup of Pa-233 which is dependent upon Φ_{th}, the thermal flux in the fission reactor. In order to avoid transient concentrations when introducing the fuel into the fission reactor, control considerations suggest this equilibrium Pa-233 concentration as the optimum concentration for the fuel to have at the end of the decay phase. Reactor physics considerations also dictate the concentration of U-233 necessary at the start of the burn phase (i.e. at the end of the decay phase).

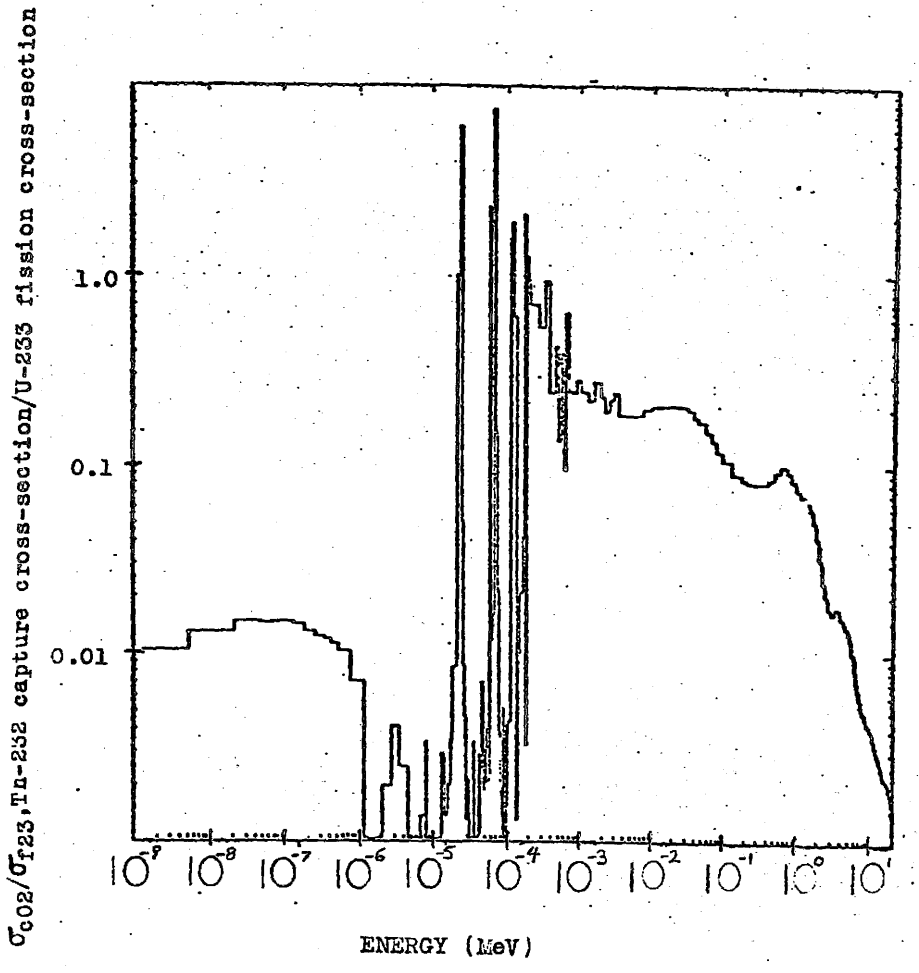

Figure 2.1-1 The ratio of Th-232 capture cross-section to U-233 fission cross-section.

Application of these two boundary conditions yields:

$$N_{13}(t=\Delta t_1).\exp(-\lambda_{13}.\Delta t_2) = \langle N_{13}\rangle_b \qquad (2.1.6)$$

$$N_{23}(t=\Delta t_1).\exp(-\lambda_{23}.\Delta t_2) + N_{13}(t=\Delta t_1).[1-\exp(-\lambda_{13}.\Delta t_2)]$$

$$= \langle N_{23}\rangle_b \qquad (2.1.7)$$

where

$$N_{13}(t=\Delta t_1),\ N_{23}(t=\Delta t_1)$$

are the concentrations of Pa-233 and U-233 at the end of the breed phase respectively, and

$$\langle N_{13}\rangle_b,\ \langle N_{23}\rangle_b$$

are the desired concentrations of Pa-233, U-233 respectively desired at the start of the burn phase; Δt_1, Δt_2 are the lengths of breed, decay phases respectively.

Analysis of the solutions of (2.1.1) and (2.1.2) show $\langle N_{13}\rangle_b \propto \Phi_{th}$ and $N_{13}(t=\Delta t_1) \propto \Phi_f$, the breeding blanket flux. The isotopic concentrations at time $t=\Delta t_1$, are dependent upon the length of the breed phase, Δt_1, the initial Th-232 concentration, N_{02}^o, and the fast neutron flux in the breeding blanket, Φ_f. Using appropriate values for N_{02}^o, Φ_f and Φ_{th}, equations (2.1.6) and (2.1.7) can then be solved for the optimum values of Δt_1 and Δt_2.

Figure 2.1-2 illustrates the sum of Δt_1 and Δt_2, as a function of Φ_f and neutron energy E_o. The increased breeding capability of the 30 keV neutrons as compared to 1 MeV and 100 keV neutrons is evident from the figure. A point to note is the asymptotic approach

Figure 2.1-2 Time for breed & decay phases as a function of neutron flux for various fast neutron energies.

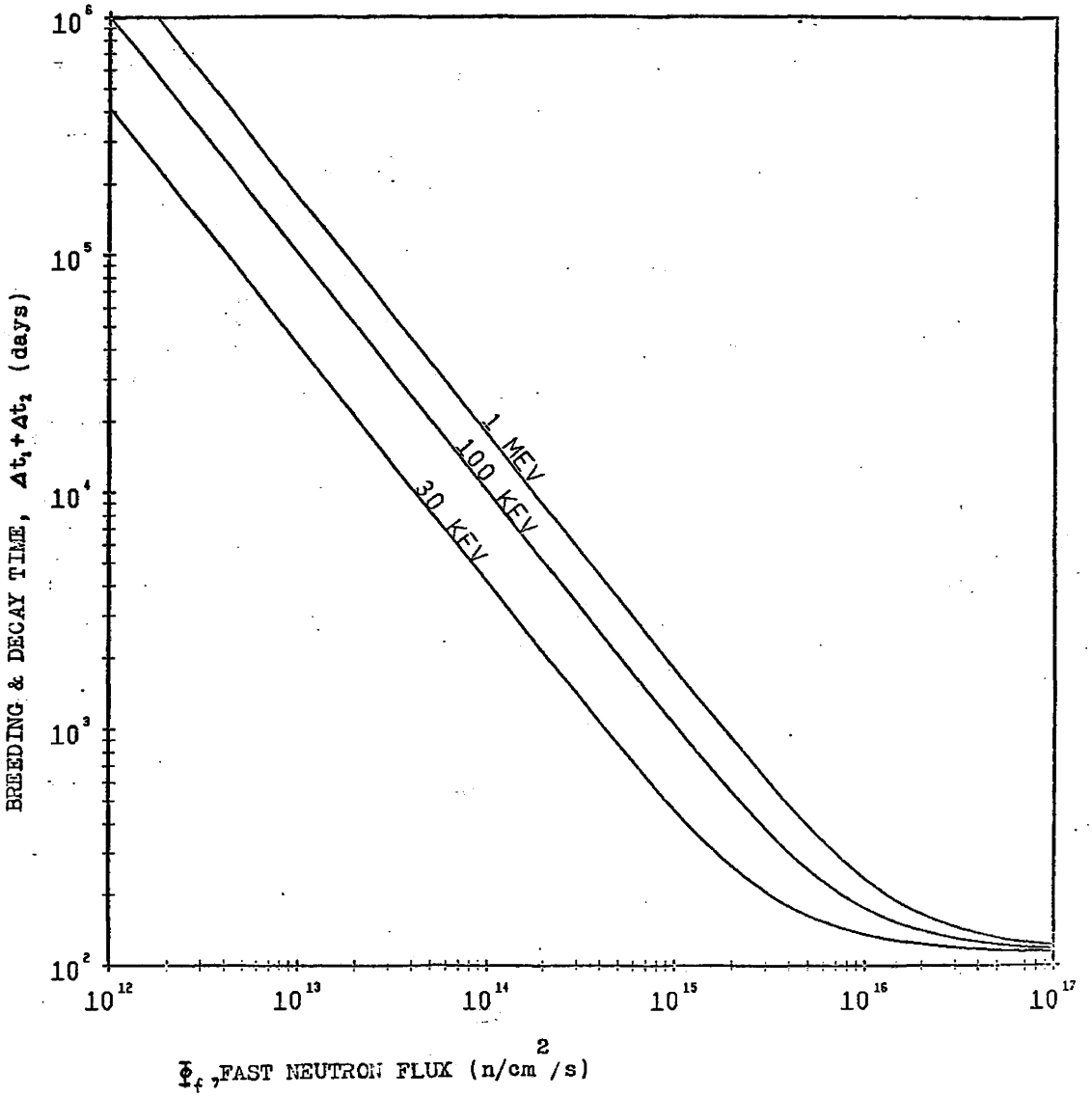

of the curves to about 100 days as Φ_f increases. The explanation for this fact is that as the fast flux increases, Δt_1 approaches zero, however Δt_2 is limited by the Pa-233 half-life of 27.4 days. The asymptotic region corresponds to the ideal situation in which one has a "lump" of Pa-233 at time zero and allows it to decay to a desired concentration of U-233.

Figures 2.1-3 and 2.1-4 illustrate the dependence of Δt_1 and Δt_2 on Φ_{th} with 30 keV neutrons in the breeding blanket. Note that the sum of Δt_1 and Δt_2 coincide for differing Φ_{th} until Φ_f reaches about 10^{15} n/cm^2/s and then is inversely proportional to Φ_{th}. The reason for the inverse proportionality is that as Φ_{th} increases, $\langle N_{13} \rangle_b$ increases thereby requiring a shorter decay phase to achieve the necessary Pa-233 concentration. Figure 2.1-5 demonstrates that no decay phase is necessary for fast fluxes below a certain value. This is because the equilibrium concentration of Pa-233 in the breeding blanket which is proportional to Φ_f, will be less than $\langle N_{13} \rangle_b$ for values of Φ_f below a certain critical value. At fast flux levels below this critical value, which is proportional to Φ_{th}, there is no need to allow Pa-233 to decay as its concentration will have to be increased in the fission reactor nonetheless.

The dependence of Δt_1 and Δt_2 on $\langle N_{23} \rangle_b$ is depicted in Figures 2.1-5 and 2.1-6. As would be expected it is apparent that increasing desired U-233 concentration increases the time required for breeding. Also note that the asymptotes fall within the range of about 100 to 150 days for substantially varied $\langle N_{23} \rangle_b$. Upon examination of Fig. 2.1-6 it is not immediately obvious why the curves start out coincidental

Figure 2.1-3 Breed & decay times as a function of fast neutron energy for various thermal flux values (note-fast neutron energy is 30keV and $\langle N_{23} \rangle_B$ is 2.0%).

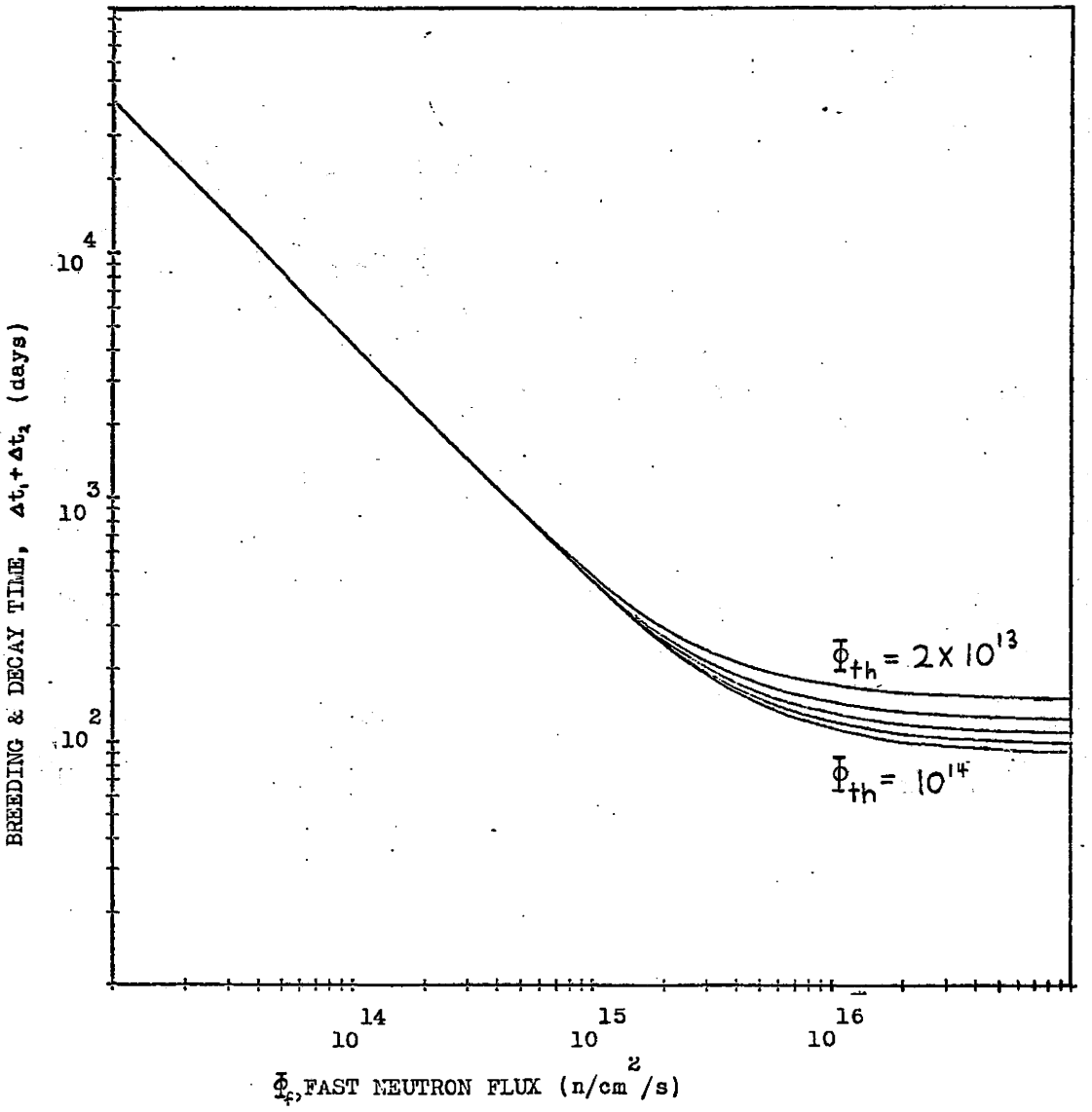

Figure 2.1-4 Decay time as a function of fast neutron flux for various thermal neutron flux. (note- fast neutron energy is 30 keV and N_{23}= 2%)

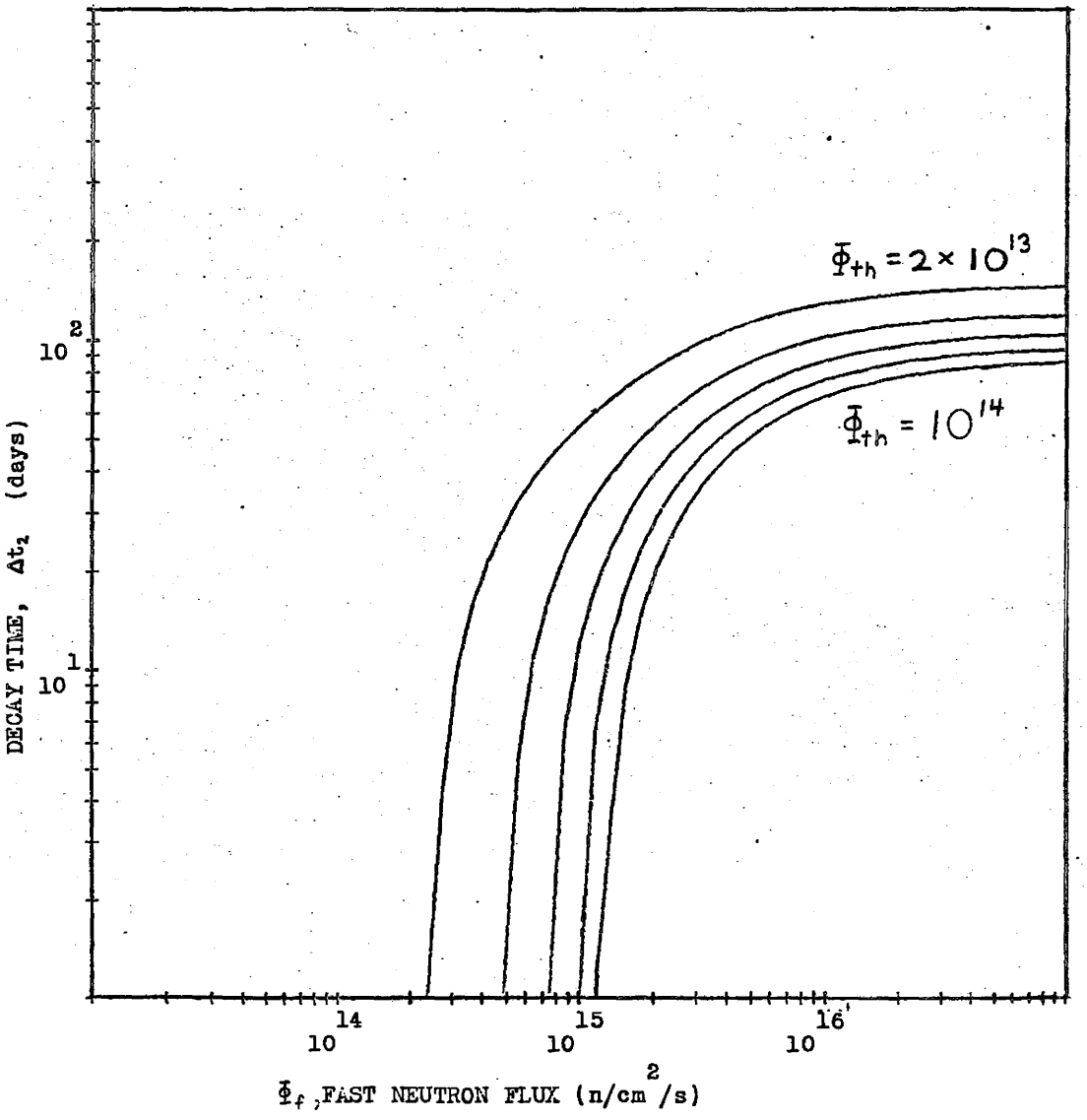

Figure 2.1-5 Breeding & decay time as a function of fast neutron flux for various $\langle N_{23} \rangle_b$ (note- thermal flux equals 5×10^{13} and fast neutron energy is 50 keV)

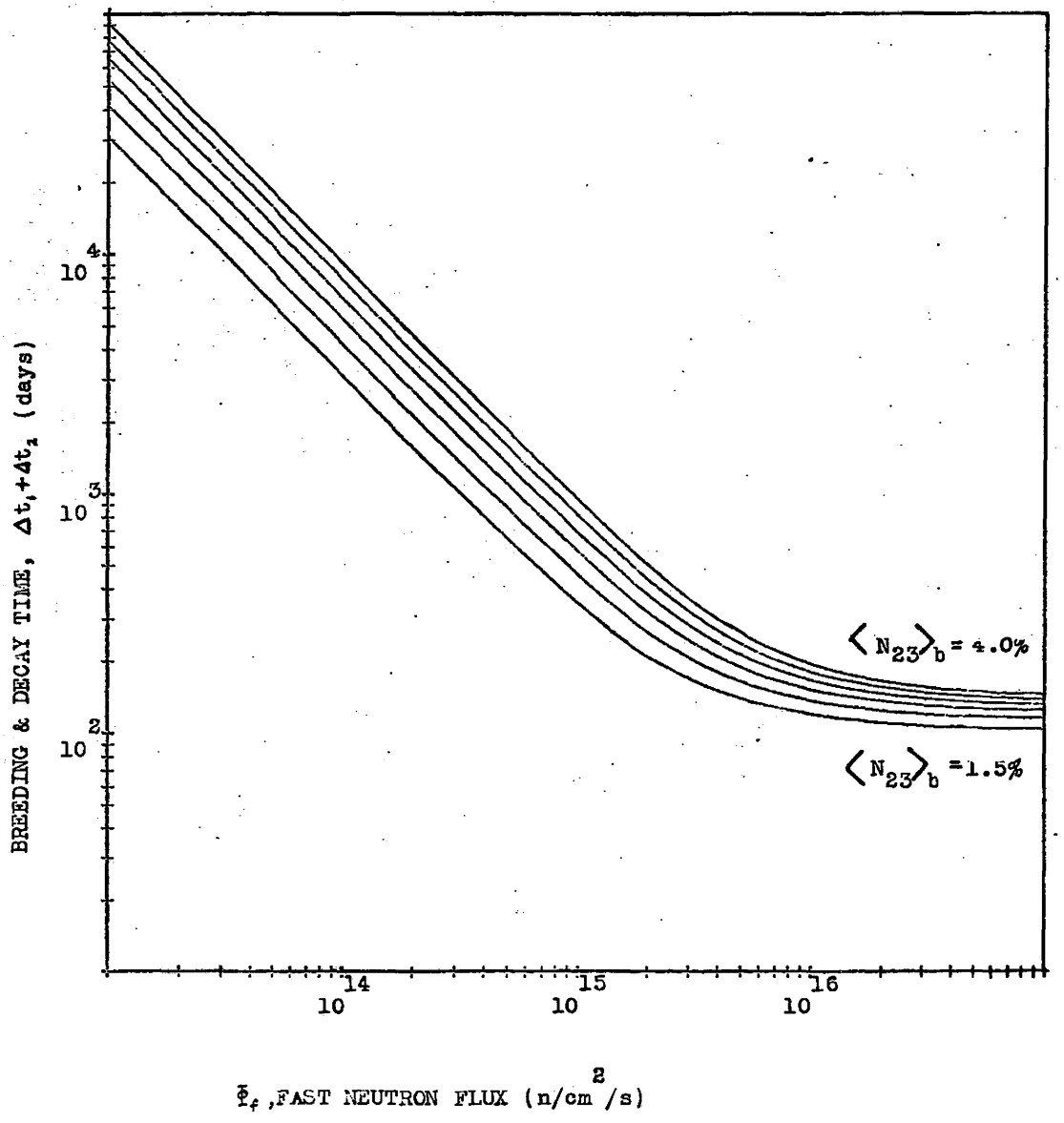

Figure 2.1-6 Decay time as a function of fast neutron flux for various $\langle N_{23} \rangle_b$ (note- fast neutron energy is 30 keV and thermal flux = 5×10^{13} n/s/cm^2)

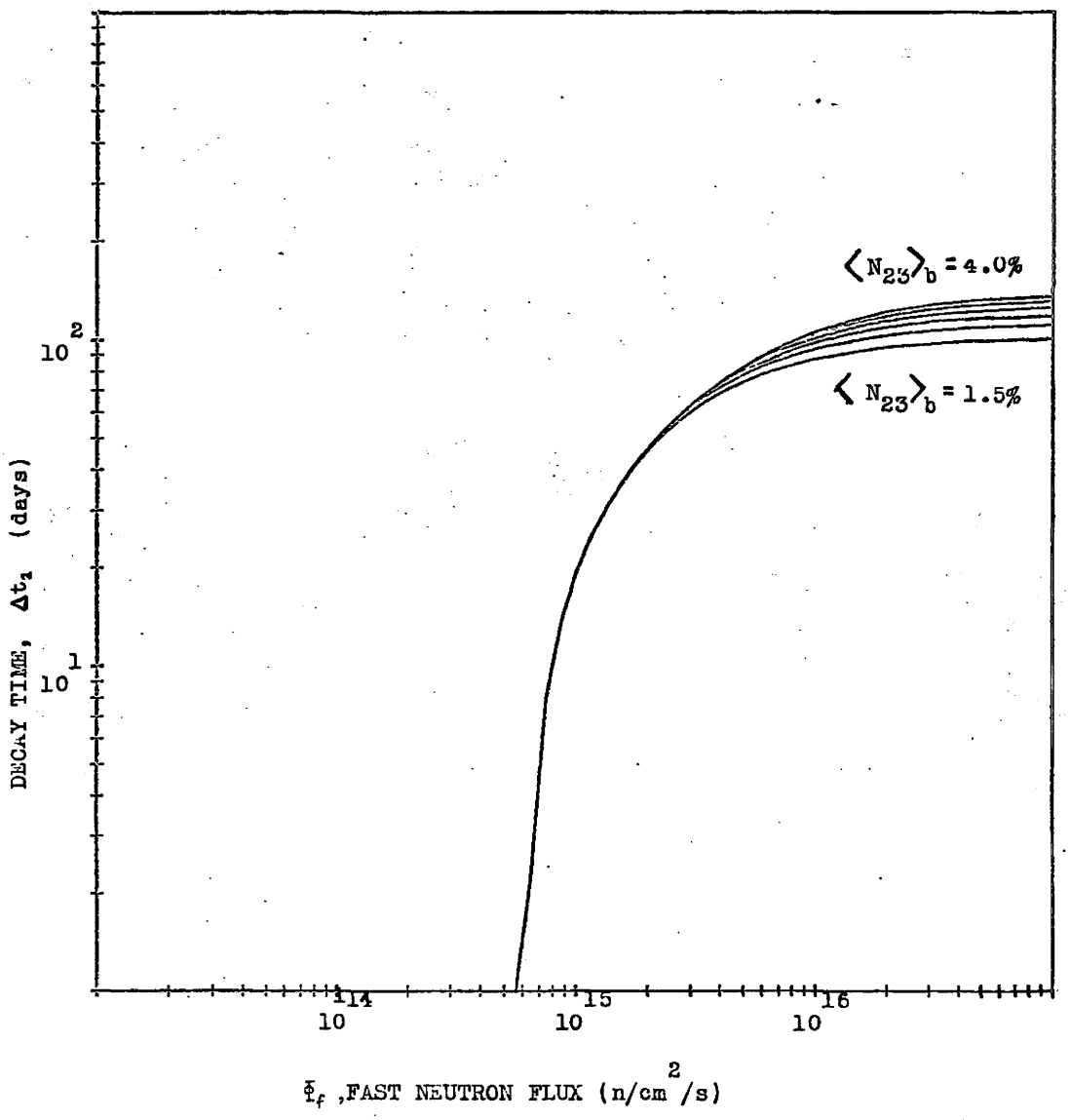

and then diverge as they approach the asymptotic region. The reason the curves have the same critical values of fast flux is that Φ_{th} is constant for each curve and the dependence of this critical value on Φ_{th} has already been mentioned. To understand the divergence recall again the "lump" of Pa-233 at time zero. If a greater value of $\langle N_{23} \rangle_b$ is called for then a greater value of N_{13} at time Δt_1 will be required also. However, keeping Φ_{th} constant implies $\langle N_{13} \rangle_b$ is constant therefore a longer decay time is necessary to reach the desired Pa-233 concentration for the fission reactor.

Another aspect of the cycle worth examining is the amount of fission power produced in the breeding blanket. This can be characterized by ρ, the specific power density. This value is defined as the fission power in the breeding blanket divided by the volume of heavy element in the blanket.

This is also given by;

$$\rho = \text{constant} \times \sum_{ij} \sigma_{ij}^{f} \Phi_f N_{ij} \qquad (2.1.8)$$

The reason for using the specific power density is again to avoid specifying the design of a breeding blanket.

The maximum value of ρ for the first two cycles is shown in Figures 2.1-7 and 2.1-8 respectively. Also shown for comparison purposes are typical outputs of a CANDU and Fast Breeder Reactor.[18] Examination of Fig. 2.1-7 reveals that for $N_{23} \gtrsim 2.5\%$, the output of, say, a CANDU is reached at about 2 to 6 x 10^{15} n/cm^2/s. Notice the levelling off which occurs. This is due to the limitation of the U-233 production rate, hence the fission rate, by the Pa-233 half-life, during the first

Figure 2.1-7 The maximum specific power density in the first breed phase as a function of fast neutron flux for various $\langle N_{23} \rangle_b$

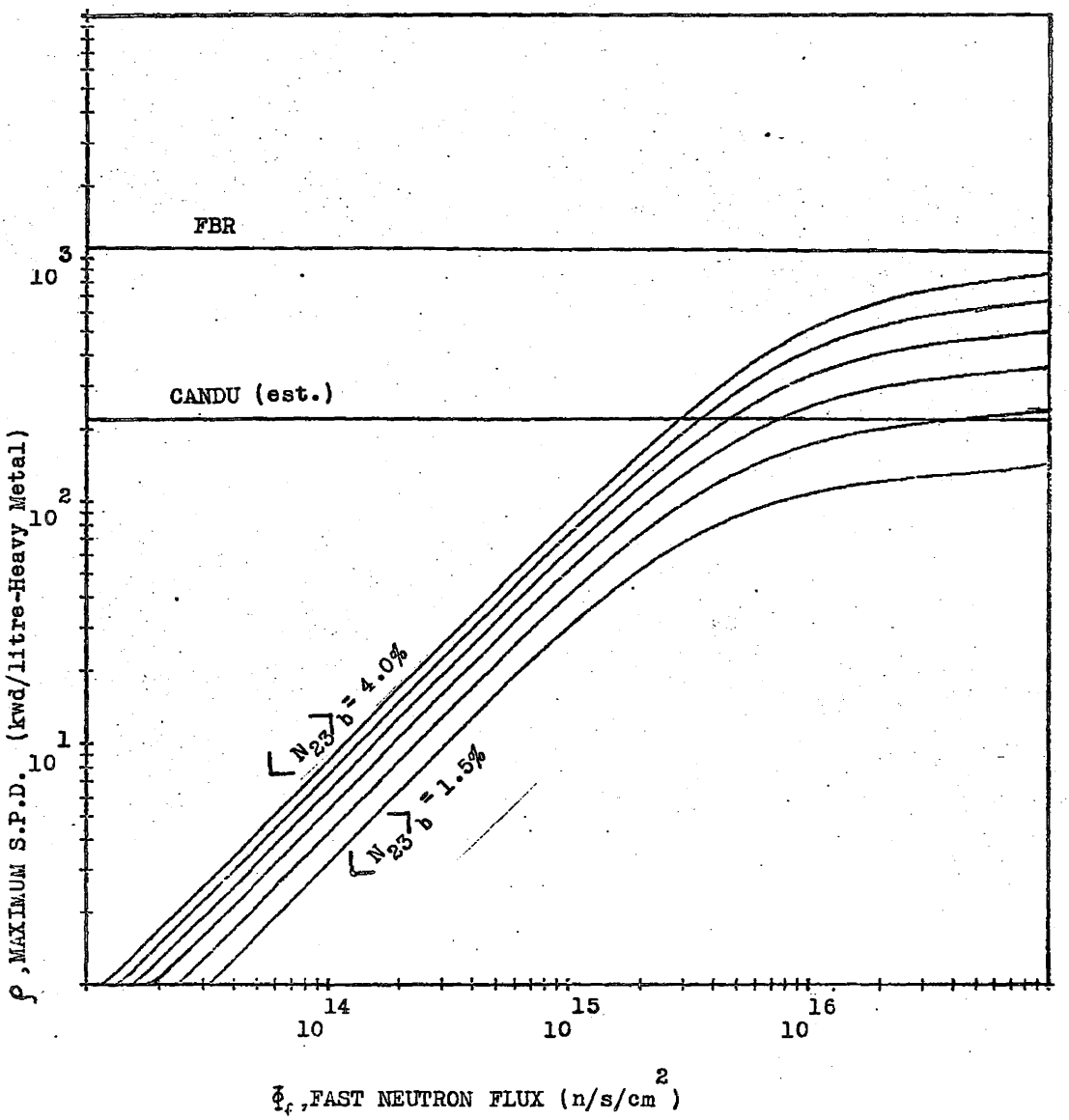

Figure 2.1-8 The maximum specific power density during the second breed phase as a function of fast neutron flux for various $\langle N_{23} \rangle_b$

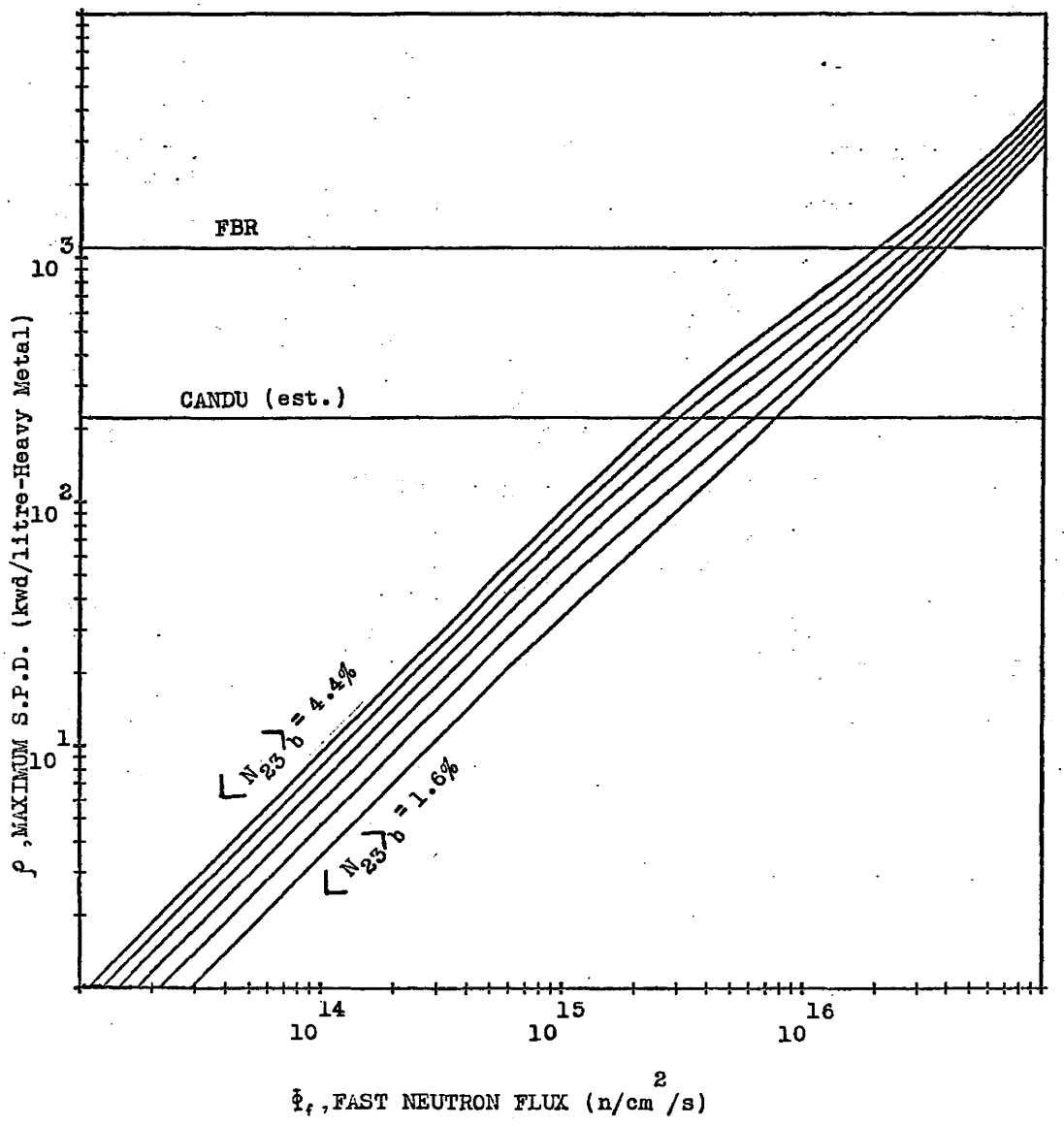

cycle. The subsequent figure does not exhibit this levelling off because substantial fissile material will be present already during the second cycle.

The foregoing may have possible useful implications in the practical utilization of the ITC. Considerable power gradients across the blanket are expected for a "homogeneously" fuelled blanket. Dealing with this type of gradient represents a novel challenge for blanket designers. Leonard[4] has suggested a fuel pin of decreasing diameter towards the neutron source as a possible solution to this problem. If the tandem cycle proposed in this thesis is utilized, another possible alternative may be to place fuel pins closer to the neutron source for the first cycle. For subsequent cycles the fuel may be placed further away from the source. In this manner the inner fuel would be limited in its power production while the outer fuel would not. This could then have the effect of smoothing the forementioned power gradient. The most practicable design could quite possibly use a combination of the two methods.

2.1.1 Summary

It would appear that the "interrupt" in the ITC could be anywhere from 0 to 100 days depending primarily upon the neutron fluxes in the breeding blanket and fission reactor. It also seems evident that this interruption will not be required unless the fast neutron flux in the breeding blanket is of the order of 2×10^{14} n/s/cm^2 or higher.

2.2 Th-232 and U-233 in CANDU Reactors

The use of Th-232 and U-233 fuel in a CANDU heavy water reactor has profound effects in the manner in which the reactor operates.[11,12,19]

As previously mentioned, U-233 is better suited for use in thermal reactors than U-235. This fact is exhibited in Fig. 2.2-1 which shows the excess neutrons produced during fission of U-233 and U-235 as functions of energy. These excess neutrons are available to produce new fissile material and make up for unavoidable absorption or losses. It is evident that U-233 has a larger η for neutrons having energy in the thermal range. This means that a neutron absorbed in U-233 will be put to better use than one absorbed in U-235.

Figure 2.2-2 illustrates this effect from a slightly different viewpoint. The value of the infinite multiplication factor k_∞ is shown for natural Uranium and also "unnatural" Uranium (i.e. all U-235 replaced by U-233). If there was such a material it would be possible to extract roughly 80% more energy from this "unnatural" Uranium due to the more efficient neutron utilization. However, the U-233 fuel in actual usage would probably contain Th-232 as opposed to U-238.

The neutron absorption cross-section of Th-232 is approximately three times that of U-238. This fact, coupled with the similar fission cross-sections for U-235 and U-233 means that substantially more fissile material must be present in a Th-U fuel for criticality as compared to that required for natural U fuel. The typical concentrations which might be observed in Th-U fuel are shown in Fig. 2.2-3.

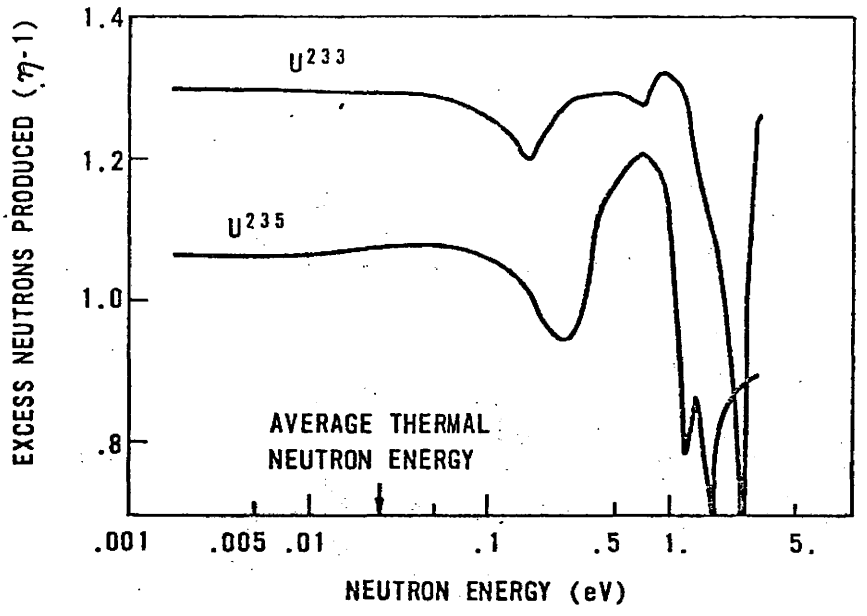

Figure 2.2-1 η-1 for U-233 and U-235 as a function of neutron energy

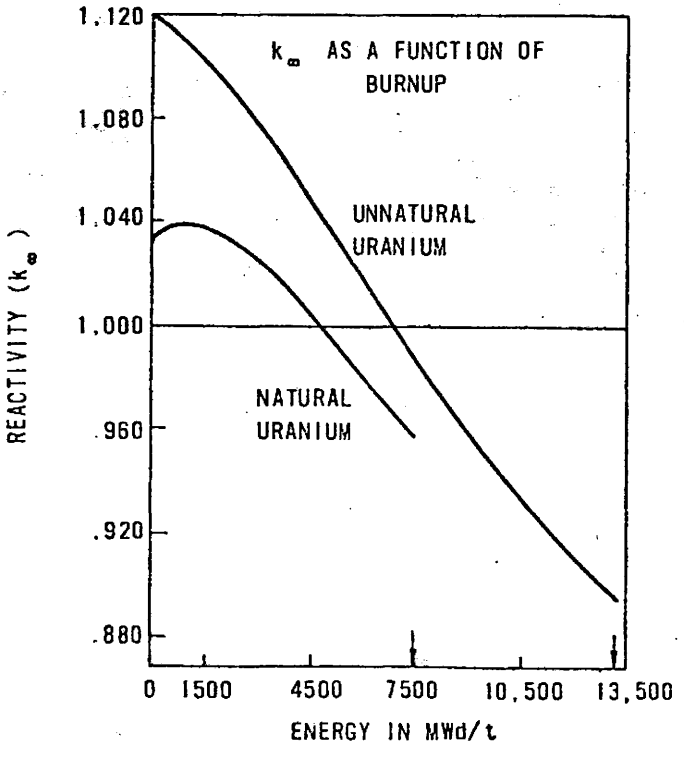

Figure 2.2-2 k_∞ as a function of burnup.

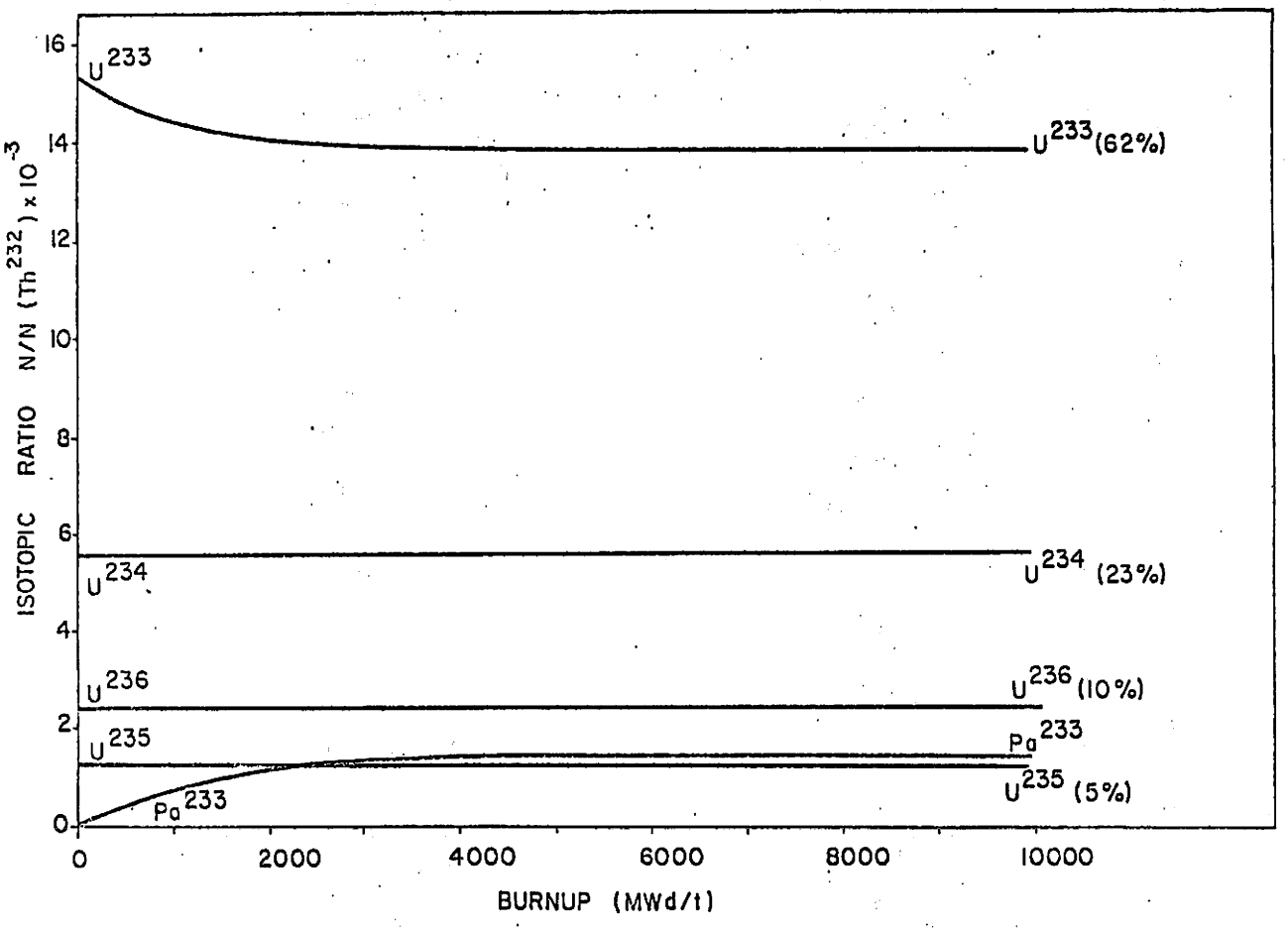

Figure 2.2-3 Typical isotopic compositions of equilibrium uranium in Th^{232}.

It is clear that about 1.5% U-233 is required here as compared to .715% U-235 found in natural U fuel.

Another consideration involved in the use of Th-U fuel is the sensitivity of burnup predictions to a 10 mk (i.e. 1%) reactivity allowance. This allowance represents uncertainty in the calculation of leakage, reactivity, or in design. Figure 2.2-4 contains the information necessary to assess this sensitivity. The figure shows that the absorption and fission cross-sections of Th-U fuel decreases initially due to the effect of Pa-233 production and that subsequently Σ_f levels out. The absorption cross-section begins to rise slowly due to the non-saturating fission product accumulation and, less significantly, to Th-232 depletion. The end result is that $\nu\Sigma_f/\Sigma_a$ decreases very slightly so that a slight reactivity increment will affect the maximum burnup prediction quite profoundly. A crude estimate of 500 MWd/Te per mk of reactivity has been put forth in this respect.[12] The implication then is that fission product calculations should be quite accurate to get a clear estimate of the maximum burnup of the fuel.

The branching of the U-233 production chain (Fig. 2.0-1) at Pa-233 leads to some interesting effects also. It is apparent that increasing the flux level will increase the capture rate in Pa-233. This in turn results in an increasing production of U-234, a non-fissile isotope, and decreased production of U-233. Hence, the reactivity of a fuel bundle decreases as the flux, or power density is increased, resulting in a lower attainable burnup of fuel for higher power densities. The variation of reactivity for two flux levels is

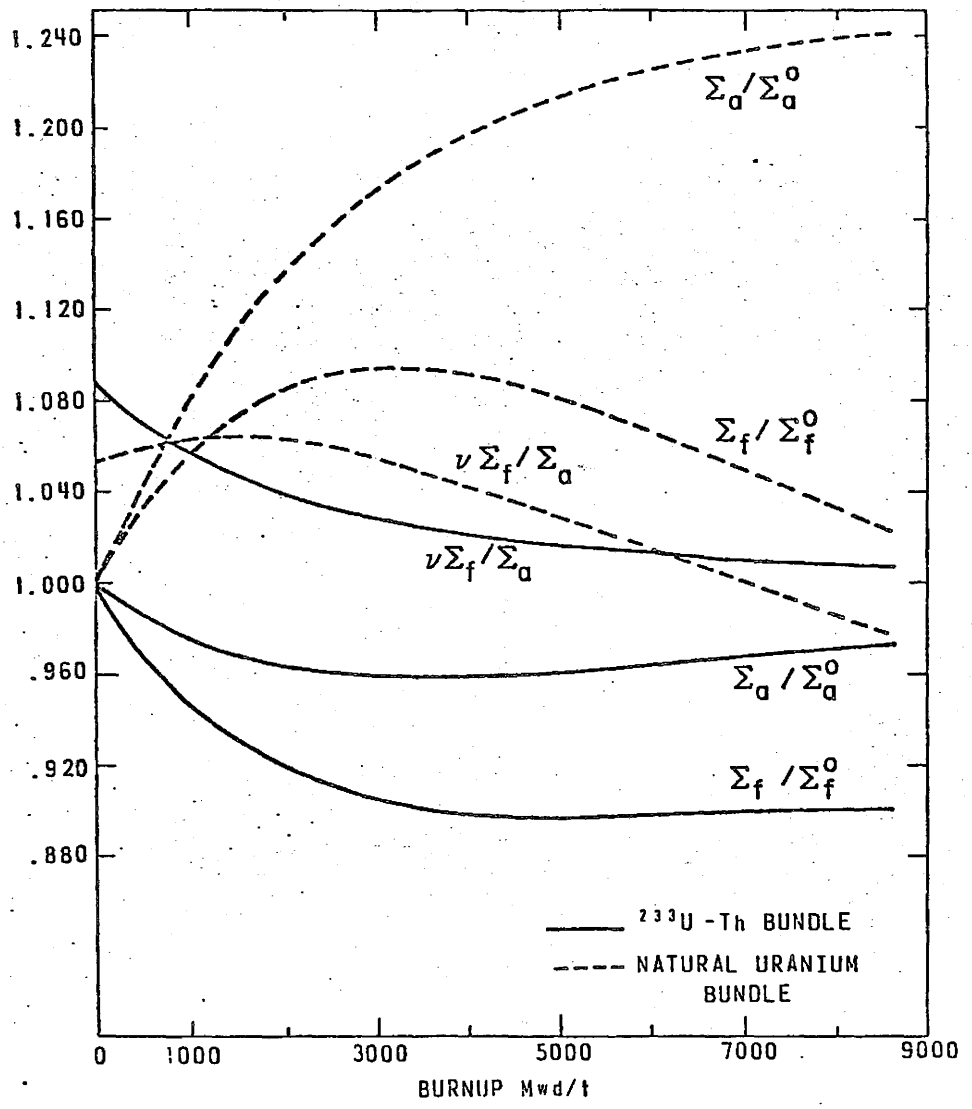

Figure 2.2-4 Normalized Σ_f, Σ_a and reactivity versus burnup.

depicted in Fig. 2.2-5. The figure shows that a 60% increase in power level produces a 47% reduction in attainable burnup due to the increased absorption of neutrons by Pa-233.

The flattening of flux distributions is also associated with the forementioned phenomenon (Fig. 2.2-6). Near the centre of the reactor where the flux is greatest the reactivity is decreased which, in turn, tends to depress the flux. The opposite effect occurs near the ends of the reactor. The net result is a flattened flux distribution, best described as a squashed cosine in the axial direction and a squashed Bessel function radially. This effect is simultaneously good and bad in that it allows for more power to be extracted from a channel relative to the natural U fuelled CANDU, however the neutron leakage at the edges of the reactor is also increased because of the increased slope of the flux shape there.

After shutting down the reactor the U-233 concentration begins to increase because of Pa-233 decay. It has been estimated[19] that after a prolonged shutdown this could result in an increased reactivity of up to 100 mk (i.e. 10%). Therefore, a substantial shutdown depth, i.e. reactivity worth of shut-off rods, would be required to compensate for this effect.

Also concerned with reactor control is the production of I-135 and Xe-135 in the reactor during normal operation. It turns out that I-135 production from U-233 fission is significantly less than from U-235 fission. This fact, coupled with the lower flux levels in the Th-U fuelled reactor, leads to a lower Xe-135 level in this reactor after shutdown. The rate of Xe-135 buildup in Th-U fuelled reactor is approximately half that found in the natural

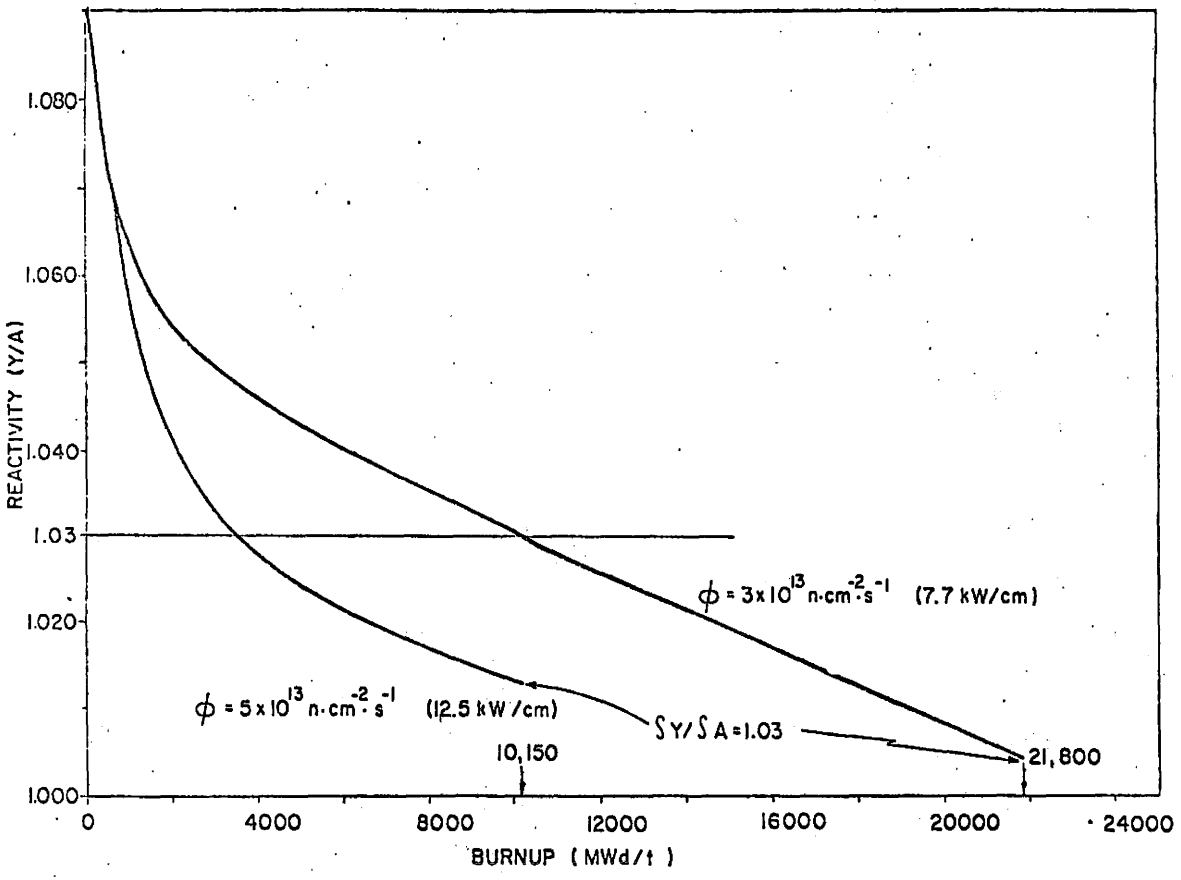

Figure 2.2-5 Variation of Reactivity with burnup at two levels of flux.

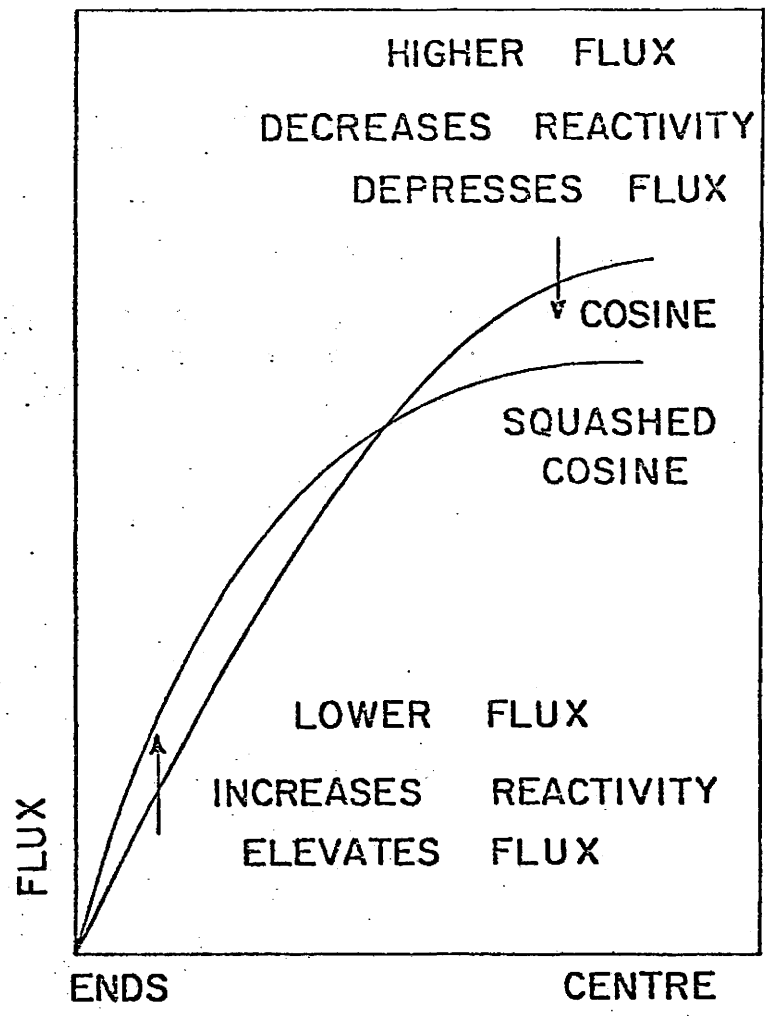

Figure 2.2-6
Qualitative explanation of flattening of flux distribution due to Pa^{233} branching.

U-reactor. This implies that less Xe-135 override capability is required in the Th-U reactor and also there is more decision/action time available after a shutdown of the Th-U reactor.

CHAPTER 3

NUCLEAR FUEL INVENTORY TRAJECTORIES OF FUSION FISSION SYMBIONTS

The previous chapter concerned itself mainly with an analysis of the fissile fuel trajectories of a Th-232, U-233 based fusion fission symbiotic system. In the discussion to follow, the emphasis will be on developing parametric analysis of fissile and fusile fuel trajectories. The effect of a fusile isotope with a short half-life (e.g. Tritium) will be investigated. The major difference in the analysis here as compared to the preceding is one of the time periods involved. The accent will be on long term effects (i.e. years) as opposed to the short-term one (i.e. days) looked at previously.

In most fusion-fission systems studies, it has become common practice to impose a time dependence on both the bred fissile fuel (i.e. ^{233}U or ^{239}Pu) and bred fusile fuel (i.e. Tritium) by a differential relationship first suggested by Lidsky[10]

$$\frac{1}{N_i(t)} \frac{dN_i(t)}{dt} = \frac{1}{\tau} = \text{constant} \qquad (3.0.1)$$

where $N_i(t)$, with i=1 or 2, represents the number of fissile or fusile atoms. This equation leads to the expression for the exponential growth rate of nuclear fuel

$$N_i(t) = N_i(0).\exp(t/\tau) \qquad (3.0.2)$$

from which parameters such as fuel doubling times are deduced.

While Eq. (3.0.1) is in a convenient mathematical form, its use, however, seems unwarranted and will in general lead to erroneous results. This point is discussed in detail in Appendix 1.

A better formulation for the nuclear fuel variation with time - that is the trajectory concept as implied herein - must include considerations associated with, for example, residence times of the bred fuel in the fusion and fission reactor blankets, radioactive decay of tritium, and the provision of an external inventory of nuclear fuel which can be used either for fuel withdrawals or deposits to ensure that the two reactors operate at a constant power level.

3.1 Systems and Isotope Description

The fusion-fission symbiont system of interest here is illustrated schematically in Fig. 3.1.1. In order to introduce sufficient generality, we specify that both tritium and fissile fuel is bred in each of the two blankets by the usual neutron induced breeding chains;[15] more simplified isotope couplings follow as special cases of this general formulation.[8] If we designate by N_1 the number of fusile fuel atoms (i.e tritium) and by N_2 the number of fissile fuel atoms (i.e. ^{233}U or ^{239}Pu) then the fusile fuel destruction rate in the D-T fusion core is given by

$$R_1 = N_D N_1 \langle \sigma v \rangle \tag{3.1.1}$$

where N_D represents the deuterium nucleus density and $\langle \sigma v \rangle$ is the suitably averaged reaction parameter; the corresponding fissile fuel destruction rate in the fission reactor may be written as

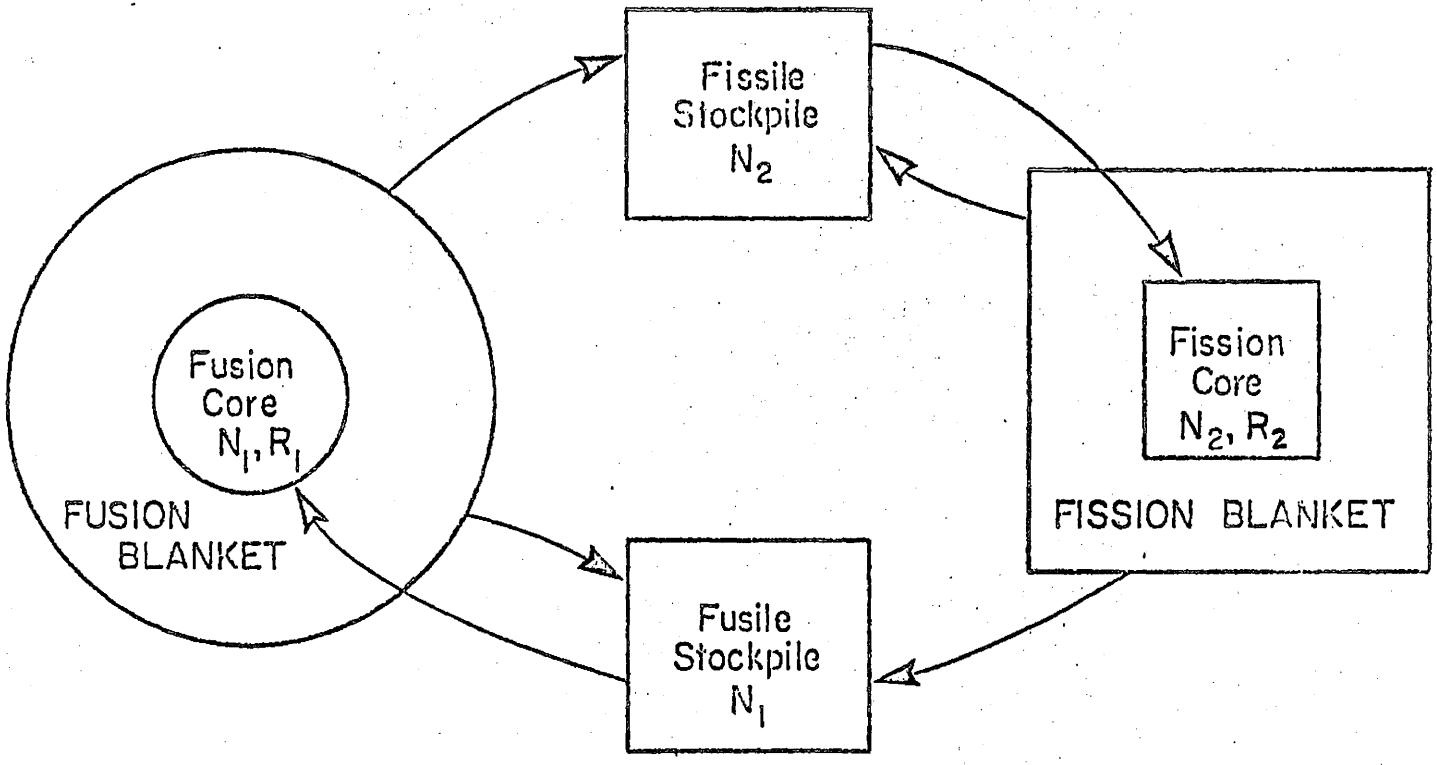

Figure 3.1-1 Schematic illustration of generalized fusion-fission symbiont.

$$R_2 = \int_j \int_E \sigma_a(E)\, N_2(\underline{r})\phi(\underline{r},E)d\underline{r}\, dE \qquad (3.1.2)$$

where $\sigma_a(E)$ is the neutron absorption cross-section for the spatially distributed fissile nucleus density $N_2(\underline{r})$ and $\phi(\underline{r},E)$ is the space and energy dependent neutron flux, the integration is carried out over all neutron energies E and the reactor volume V. The power level for each of the two reactors is given by

$$P_i = R_i\, U_i \qquad (3.1.3)$$

where U_i is the average nuclear energy released per reaction of type i. Since U_i is a constant, a constant power level requires that R_i be a constant.

As suggested in Fig. (3.1-1) an external stockpile of nuclear fuel can be envisaged as being associated with each of the fusile (i=1) and fusile (i=2) fuels. Since these nuclei are consumed in their respective cores and can be bred in both blankets, we write the variation with time of the fuel inventory of either stockpile, that is the respective fuel trajectory, as

$$\frac{dN_{i,ext}(t)}{dt} = \left[\frac{dN_i(t)}{dt}\right]_c + \sum_{j=1}^{2} \left[\frac{dN_i(t)}{dt}\right]_{Bj} - \lambda_i N_{i,ext}(t) \qquad (3.1.4)$$

where

$$\left[\frac{dN_i(t)}{dt}\right]_c = \begin{cases} \text{net destruction rate of fuel isotope i in the} \\ \text{corresponding reactor (fusion or fission)} \\ \text{core} \end{cases}$$

$$\left[\frac{dN_i(t)}{dt}\right]_{Bj} = \begin{cases} \text{net supply rate of fuel isotope i} \\ \text{extracted from the blanket of the j} \\ \text{reactor} \end{cases}$$

λ_i = radioactive decay constant of i fuel isotope

The initial conditions for Eq. (3.1.4) are

$$N_{i,ext}(0) = \text{(original stockpile inventory)} - \text{(initial core loading)}$$

$$= N_{i,ext}(0^-) - N_{i,o} \tag{3.1.5}$$

For the fuel associated with each core;

$$\left[\frac{dN_i(t)}{dt}\right]_c = \beta_i R_i \quad -1 \leq \beta_i \leq 0 \tag{3.1.6}$$

where β_i, the constant of proportionality, averaged over the reactor lifetime, is essentially the net core breeding gain. The nuclear contributions from the blankets to the stockpile inventory may be written as

$$\left[\frac{dN_i(t)}{dt}\right]_{Bj} = \frac{N_{ij}(t - \Delta t_h)}{\Lambda_{ij}} \tag{3.1.7}$$

where Λ_{ij} is the mean residence time of the bred fuel i, in the blanket of reactor j, $N_{ij}(t)$ is the corresponding inventory of the i bred fuel in the blanket j at time t; Δt_h is the hold up time of fuel discharged from the blanket, including cooling, reprocessing, etc., until it can be added to the stockpile. Clearly, the function $N_{ij}(t)$ must satisfy

$$\frac{dN_{ij}(t)}{dt} = \gamma_{ij} R_j - \frac{N_{ij}(t)}{\Lambda_{ij}} - \lambda_i N_{ij}(t) \tag{3.1.8}$$

with an initial blanket inventory of

$$N_{ij}(0) = N_{ij}^{o} \tag{3.1.9}$$

Generally, $N_{ij}^{o} = 0$ for i=1. In Eq. (3.1.8) the parameter γ_{ij} is, in effect, a nuclear fuel yield ratio - a term analogous to the widely used breeding gain; the subscript i identifies the fuel and j identifies the reactor.

With the parameters β_i, γ_{ij}, and λ_{ij} considered constant, Eq. (3.1.8) yields upon integration;

$$N_{ij}(t) = \frac{\gamma_{ij}\Lambda_{ij}R_j}{1+\lambda_i\Lambda_{ij}} \cdot \left\{1 - \left[1 - \frac{N_{ij}^{o}(\lambda_i + 1/\Lambda_{ij})}{\gamma_{ij} R_j}\right] \cdot \exp\left[-t.(\lambda_i + 1/\Lambda_{ij})\right]\right\} \tag{3.1.10}$$

substitution in (3.1.8) gives;

$$\frac{dN_{i,ext}(t)}{dt} = \beta_i R_i + \sum_{j=1}^{2} \left[\frac{\gamma_{ij}R_j}{1+\lambda_i\Lambda_{ij}}\right] \cdot \left\{1-\left[1 - \frac{N_{ij}^{o}(\lambda_i+1/\Lambda_{ij})}{\gamma_{ij} R_j}\right] \times \exp\left[-(t-\Delta T_h).[\lambda_i+1/\Lambda_{ij}]\right]\right\} - \lambda_i N_{i,ext}(t) \tag{3.1.11}$$

for

$$i = 1,2$$

Using the initial conditions specified by Eq. (3.1.5), the equation for external inventory is

$$N_{i,ext}(t) = [N_{i,ext}(0^-) - N_{i,o}].\exp(-\lambda_i t) + \frac{\beta_i R_i}{\lambda_i}[1-\exp(-\lambda_i t)$$

$$+ \sum_{j=1}^{2} [\frac{\gamma_{ij} R_j}{1+\lambda_i \Lambda_{ij}}].\{\frac{1-\exp(-\lambda_i t)}{\lambda_i} - \Lambda_{ij}.\exp(-\lambda_i t).$$

$$.[1-\exp(-t/\Lambda_{ij})].\exp[\Delta t_h(\lambda_i + 1/\Lambda_{ij})]$$

$$.[1 - \frac{N^o_{ij}(1 + \lambda_i \Lambda_{ij})}{\gamma_{ij} R_j}]\} \qquad (3.1.12)$$

Obviously, there is a substantial difference between this more correct equation and the currently widely used expression, Eq. (3.0.2).

3.2 Nuclear Fuel Trajectories

Equation (3.1.12) can be simplified somewhat for specific applications. In the case of fusile fuel, applying the assumptions $\Delta t_h \to 0$ and $N^o_{11} = N^o_{12} = 0$ gives

$$N_{1,ext}(t) = [N_{1,ext}(0^-) - N_{1,0}].\exp(-\lambda_1 t) + \beta_1 R_1 [1 - \exp(-\lambda_1 t)]$$

$$+ \sum_{j=1}^{2} \{\frac{\lambda_{ij} R_j}{1+\lambda_1 \Lambda_{1j}} \frac{1-\exp(-\lambda_1 t)}{\lambda_1} + \Lambda_{ij}.\exp(\lambda_1 t)$$

$$. [\exp(-t/\Lambda_{1j}) - 1]\} \qquad (3.2.1)$$

The corresponding expression for the fissile trajectory follows by using $\lambda_2 \to 0$ and $\Delta t_h \to 0$ and $N^o_{22} = N^o_{11} = 0$ in Eq. (3.1.12);

$$N_{2,ext}(t) = [N_{2,ext}(0^-) - N_{2,0}] + \beta_2 R_2 t$$

$$+ \sum_{j=1}^{2} \gamma_{2j} R_j \{t + \Lambda_{2j} [e^{-t/\Lambda_{ij}} - 1] \qquad (3.2.2)$$

It is informative to explore some general characteristics of the non-linear fusile, Eq. (3.2.1), and fissile, Eq. (3.2.2), fuel trajectories. As previously stated, these fuel trajectories describe the amount of fuel in the two associated stockpiles and, as indicated, this fuel inventory is composed of three components: (i) the fuel initially placed into the stockpile prior to reactor start-up, (ii) the fuel withdrawn with time as required to maintain a constant power output, and (iii) the bred fuel deposited into the stockpile. As described in the derivations, fuel consumption, breeding, hold-up due to residence times and, as appropriate, radioactive decays are all included.

While the details of the trajectories will clearly depend upon the specific numerical values of the parameters, the general and dominant features can be conveniently displayed as shown in Fig. 3.2-1.

First, consider the fuel trajectories, curves (A) and (B) of Fig. 3.2-1. Note that for a t sufficiently large, the exponential terms of Eq. (3.2.2) vanish leading to a linear asymptote,

$$N_{2,ext}(t >> \Lambda_{21}, \Lambda_{22}) \sim [\gamma_{21} R_1 + (\beta_2 + \gamma_{22}) R_2] t \qquad (3.2.3)$$

While R_1, R_2, γ_{21}, and γ_{22} are clearly positive, the core breeding gain, β_2, will by our definition be clearly negative, $-1 \leq \beta_2 \leq 0$; this notwithstanding, the magnitude of γ_{22} and γ_{21} and an appropriate fusion-to-fission power ratio would normally be chosen such that

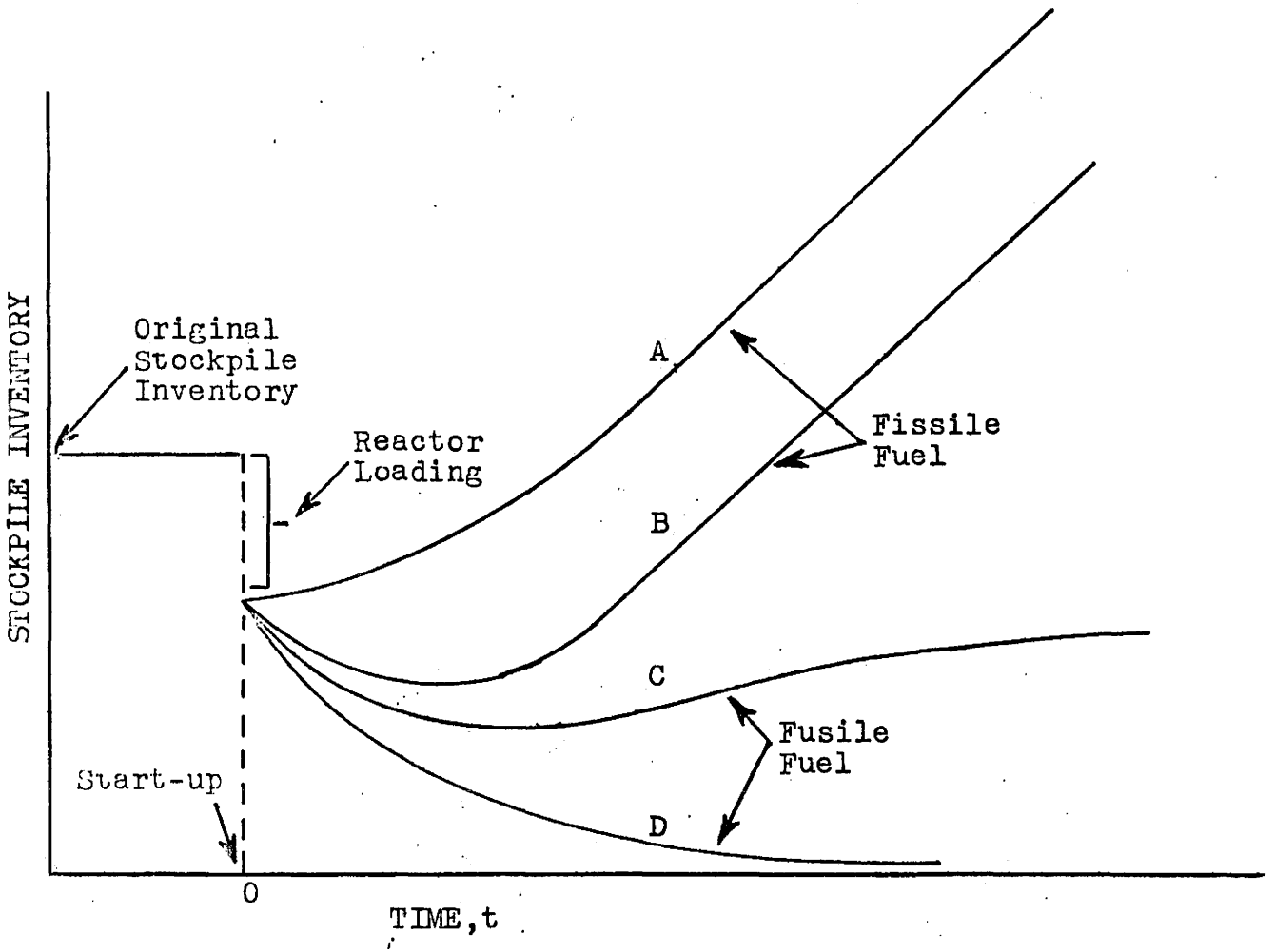

Figure 3.2.1 Graphical depiction of fuel trajectories

the trend will eventually be positively increasing, indeed; this may be viewed as a condition for the system to be a breeder of fissile fuel.

Trajectory (B) of Fig. 3.2-1 illustrates the effect of increasing mean residence times Λ_{21} and Λ_{22}; the greater these residence times, the greater the initial transient depression and hence an increasing external supply of fissile fuel is attained. The time at which the minimum extention occurs is found by setting $dN_2/dt = 0$ which in general yields a transcendental equation for ${}_2t_{min}$; a simpler equation for ${}_2t_{min}$ results if fissile fuel is bred in only the fusion blanket.

$$ {}_2t_{min} = \Lambda_{21} \cdot \log \frac{\gamma_{21} R_1}{\beta_2 R_2 + \gamma_{21} R_1} \tag{3.2.4} $$

Also, in the limit of $\Lambda_{21} = \Lambda_{22} \to 0$, no transient depression occurs and the minimum fissile inventory occurs at $t = 0$.

In each case, all fissile trajectories attain the same asymptote, Eq. (3.2.3).

The fusile fuel inventory trajectory, curves (C) and (D), display some distinct characteristics. For time t_c such that

$$ t_c \gg \Lambda_{11}, \lambda_{12}, 1/\lambda_1 \tag{3.2.5} $$

the tritium inventory attains a constant value, N_c

$$ N_c = \frac{1}{\lambda_1} \{\beta_1 R_1 + \sum_{j=1}^{2} \frac{\gamma_{ij} R_j}{1+\lambda_1 \Lambda_{ij}} \} \tag{3.2.6} $$

This constant can, by appropriate systems design, be specified to be zero at some time, curve (D) of Fig. 2, or some other specified value equal to that required to start-up a new reactor, curve (C).

In general the considerations included in this analysis lead to nuclear fuel trajectories, Eq. (3.2.1) and Eq. (3.2.2), as displayed in Fig. 3.2-1), which differ substantially from the simple exponential Eq. (3.0.2) widely used in current fusion-fission studies.

As an aside the formalism developed may be used for a solely fission breeder reactor by elimination of all terms connected with the fusion fuel/reactor in the equations for the fissile trajectories. The fissile trajectory then becomes equivalent to that developed previously.[20]

3.3 Comparative Analysis

While there may very well be substantial differences in the process assumed in a formulated mathematical description of the fuel trajectories, it is still necessary to determine if the additional detail contributes significantly to the eventual system performance characteristization. A comparison needs to be undertaken therefore based on the use of common parametric descriptions of a specific system.

For comparative purposes the fissile fuel trajectory for a system concept proposed by Blinkin and Novikov[13] has been selected. This is one of the most recent systems proposed and provides the analytical expressions and - either directly or indirectly - the data required for a comparison.

The Blinkin-Novikov (BN) systems concept is schematically illustrated in Fig. 3.3-1. It consists of a Tritium producing molten salt fission reactor coupled to a D-T fusion reactor which breeds

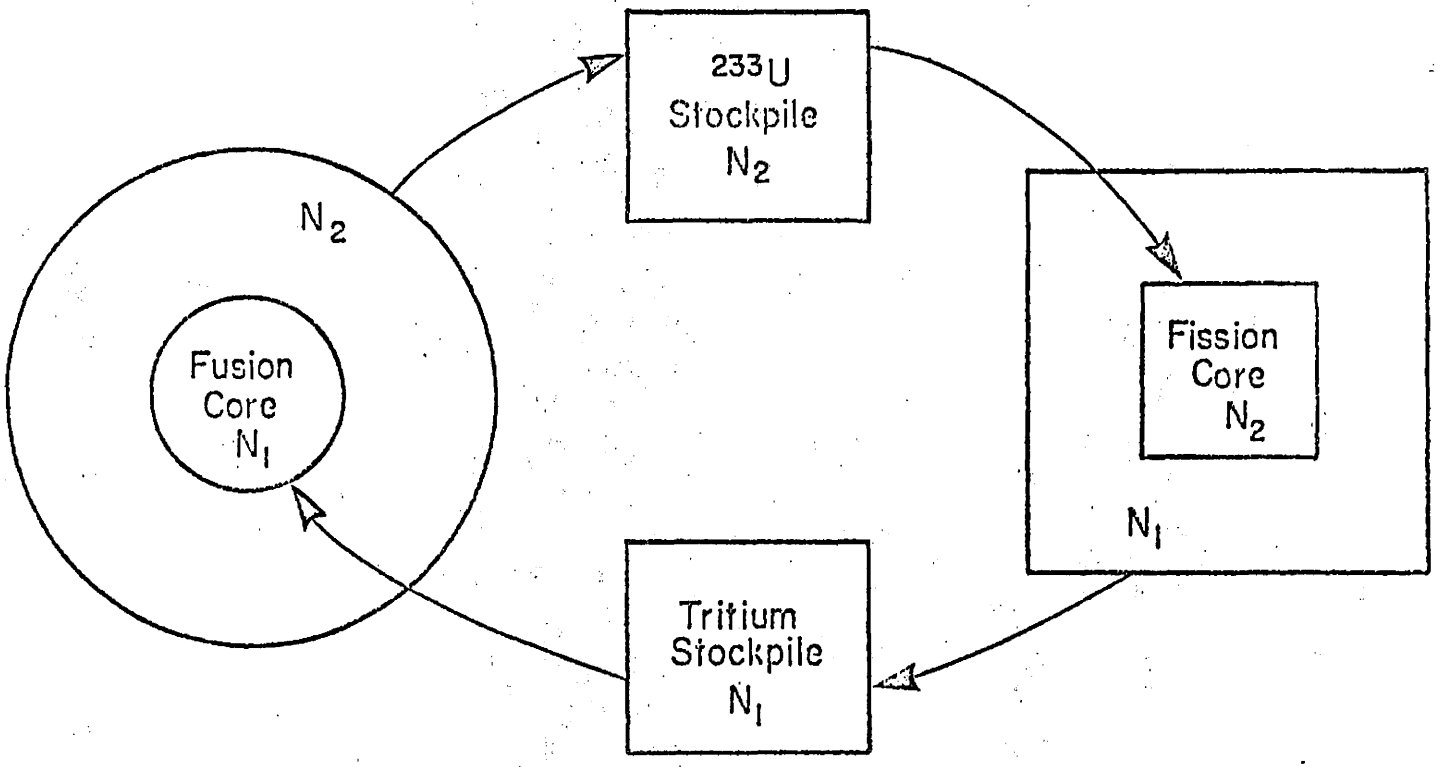

Figure 3.3-1
Schematic illustration of the Blinkin-Novikov systems concept some proposed details are the following: molten salt fusion blanket (ThF_4 ~ 27%, BeF_2 ~ 2%, N_aF ~ 71%); molten salt fission reactor ($^{239}UF_4$ ~ 1%, LiF ~ 50%, BeF_2 ~ 50%, $^6L/^7Li$ ~ 0.1%); P_1 ~ 225 MW_t; P_L ~ 2250 MW_t.

U-233 in a ThF_4 blanket; no fissile fuel breeding is assumed to take place in the fission reactor and no tritium is bred in the fusion blanket. The parameters applicable to our analytical formulation, Eqs. (3.2.1) and (3.2.2), for the four distinct variations of the same fusion-fission symbiont were extended directly or calculated from related information[13] and are displayed in Table (3.3.1). The Blinkin-Novikov fuel trajectories follow from their calculations of fuel doubling times associated with the specific exponential variation with time;

$$N_2(t) = N_2^o \exp(t/\tau)$$

The comparison between the Blinkin-Novikov fuel trajectories are shown in Figs. 3.3-2 to 3.3-6. For reasons of generalization we have normalized all results to 100% load factor. Further the fuel inventories have been normalized to units of initial reactor fuel-charge requirements; that is, the initial stockpile inventory was specified to contain two units of fuel before reactor start-up from which one unit was then removed to load the reactor with the remaining unit available for possible make up requirements. The fuel inventories are shown only after reactor loading, (i.e. for $t > 0$).

In the Blinkin-Novikov paper the value of G_{10}, specific fuel charge for the fusion reactor, was quoted as lying in the range one to six g/MW(th), therefore the two bounding values were used in separate calculations. The paper also used 20 MeV released per fusion reaction so calculations were also done with 17.6 MeV per fusion reaction.

TABLE 3.3-1

Parametric values for ^{233}U trajectory formulation developed here as applicable to the Blinkin-Novikov[13] system proposal. In addition to the listed parameters, the following data apply: $\Lambda_{12} = 3.5(s)$, $\Lambda_{21} = 120(s)$ $\beta_1 = \beta_2 = -1$, $\gamma_{11} = \gamma_{22} = 0$.

Case	γ_{12}	γ_{21}	P_1/P_2
1	0.912	1.3	0.10
2	0.847	1.4	0.094
3	0.837	1.5	0.0925
4	0.827	1.6	0.091

Figure 3.3-2 Fissile fuel trajectories for G10 equal to 1/3 g/Mw ; U2/U1 equal 200/20.

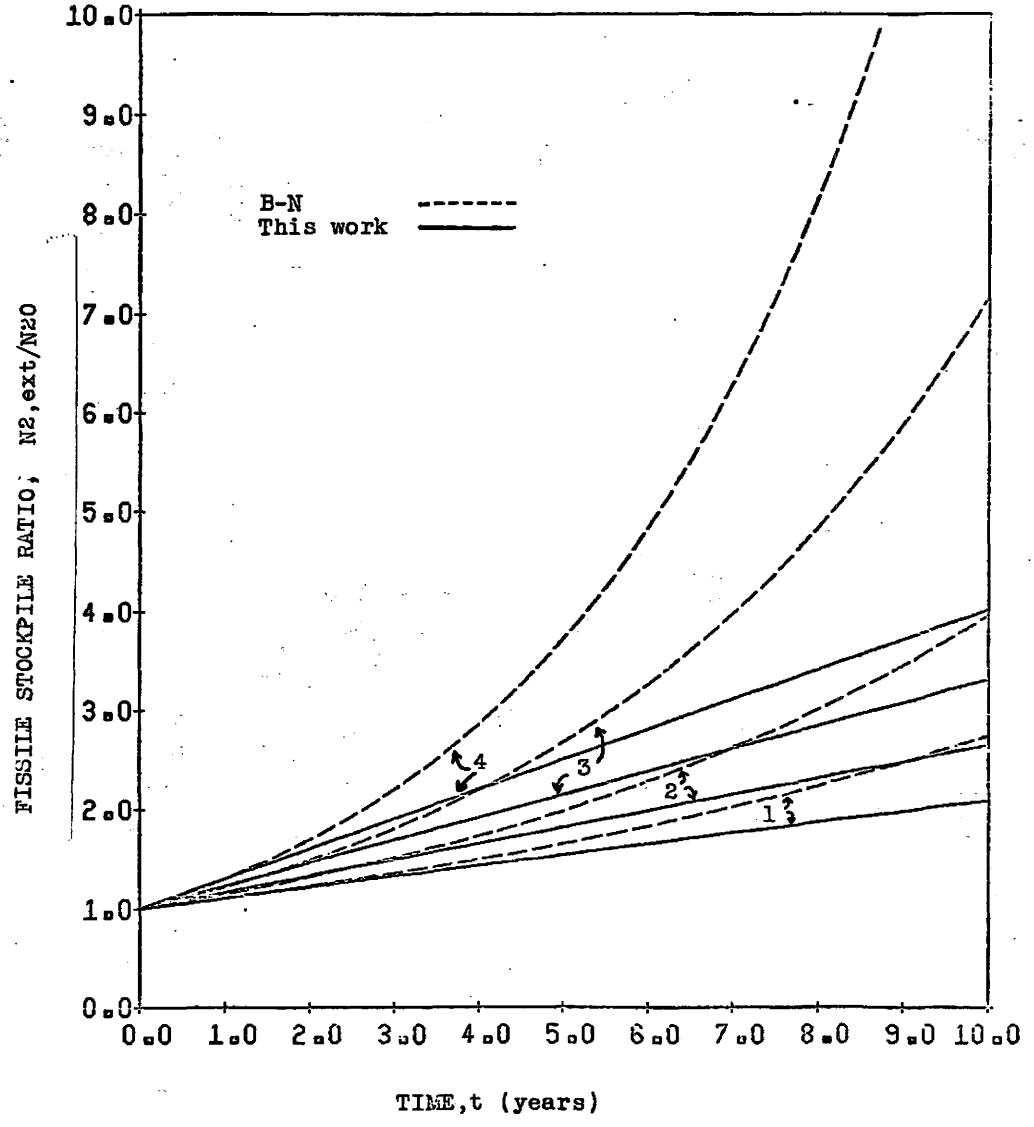

Figure 3.3-3 Fissile fuel trajectories for G10 equal 1/3 g/Mw ; U2/U1 equal 200/17.6.

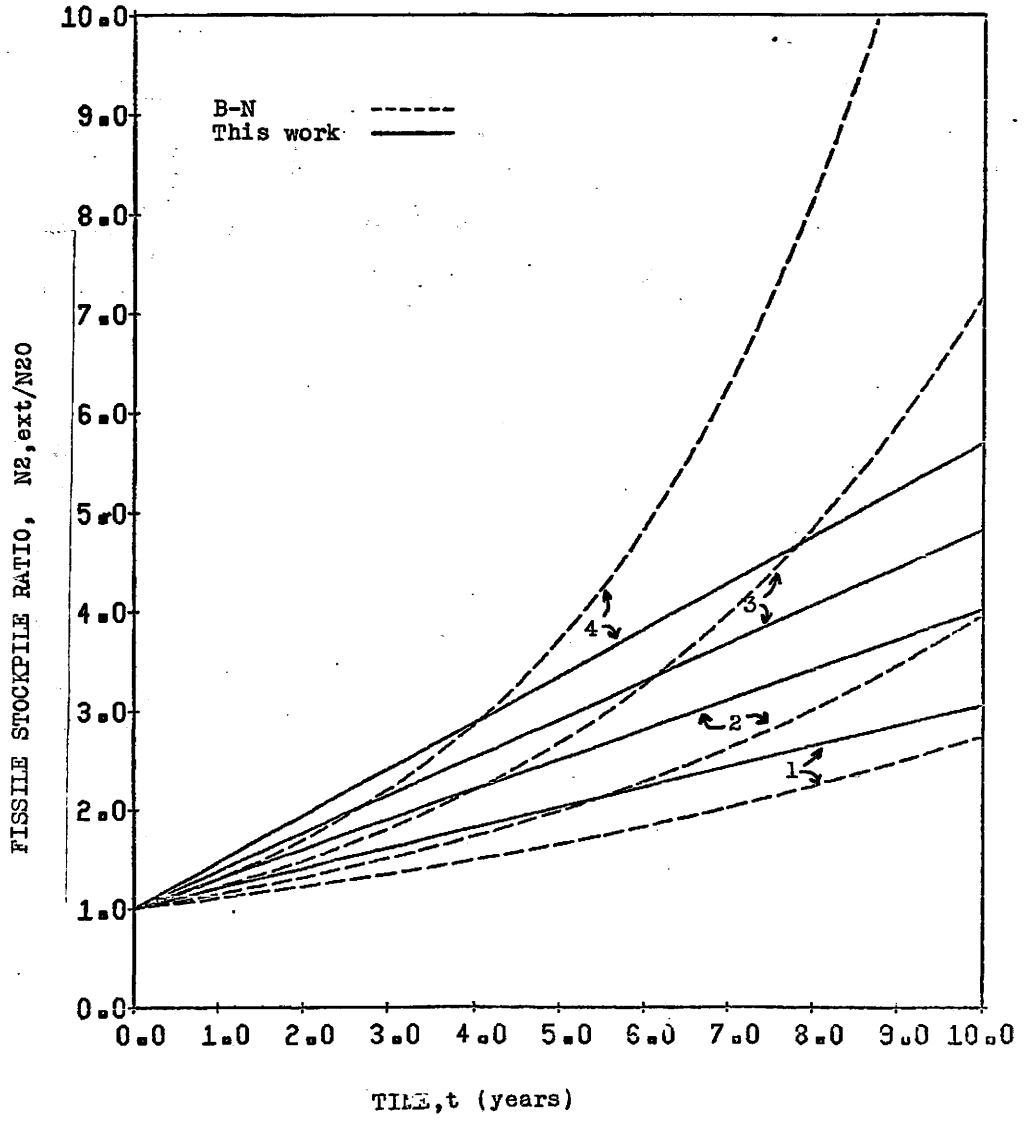

Figure 3.3-4 Fusile fuel trajectories for G10 equal 1/3 g/Mw and U2/U1 equal 200/20.

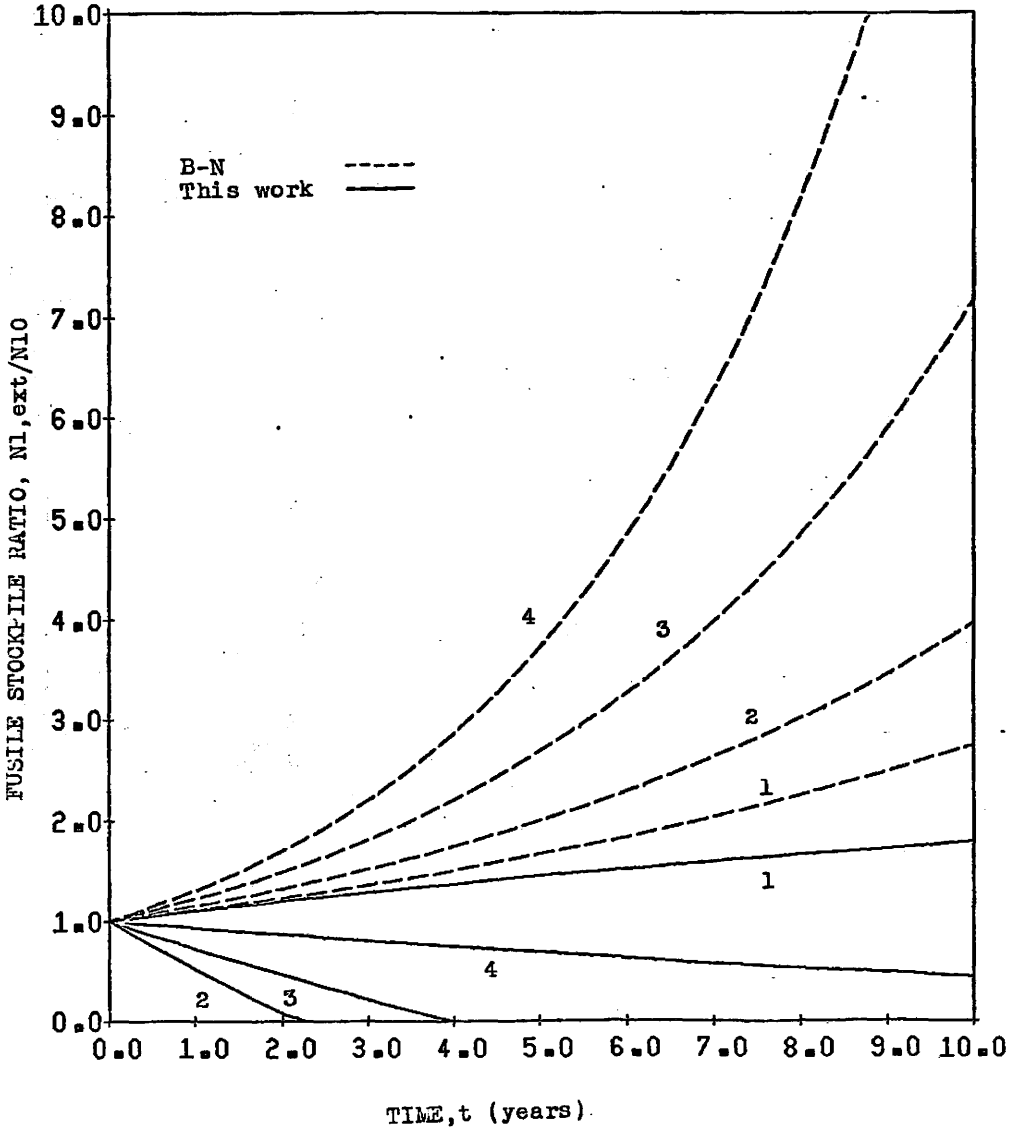

Figure 3.3-5 Fusile fuel trajectories for G10 equal 2 g/Mw and U2/U1 equal 200/20.

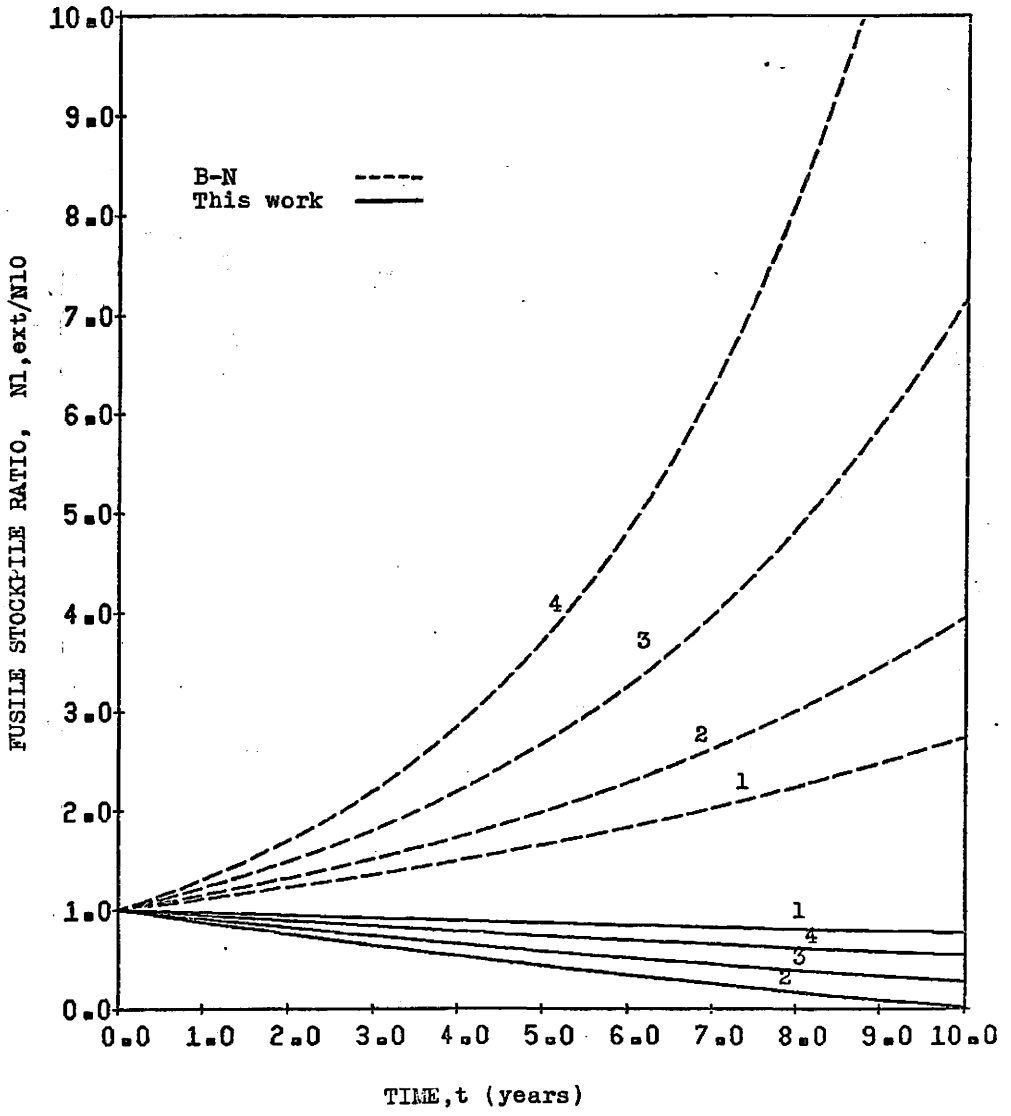

Figure 3.3-6 Fusile fuel trajectories for G10 equal 1/3 g/Mw and U2/U1 equal 200/17.6

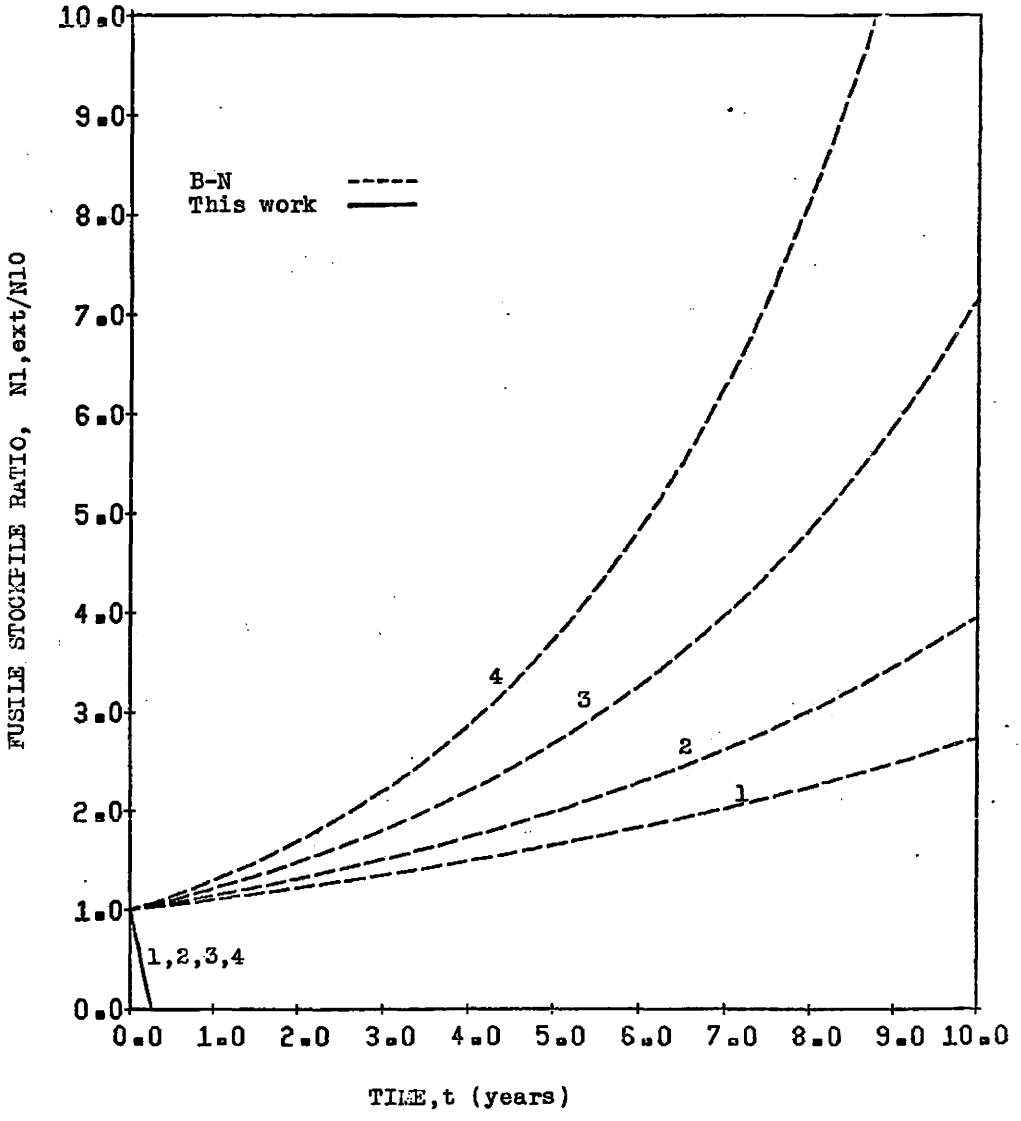

Examination of the Figures (3.3-2,3) for the fissile fuel trajectories reveals the optimism inherent in the exponential assumption. For the curves in Fig. 3.3-2 the exponential trajectories begin to over-estimate after two years and depending on the system specifics deviate more or less significantly after 10 years.

Figure 3.3-3 exhibits the same trajectories for U_1 (energy released per fusion) equal to 17.6 MeV. Since the fusion/fission powers are fixed this implies a faster fusion rate than the former case thereby increasing the rate of fissile fuel production in the fusion reactor. Thus, the exponential trajectories surpass the others at somewhat later periods ranging from about 4 to 15 years. The point to emphasize is that the exponential trajectories are highly optimistic once they cross the trajectories found here.

The fusile fuel yields are depicted in Figs. 3.3-4, 3.3-5 and 3.3-6. For these cases the optimism of the exponential trajectories is much more pronounced with only one case of 12 actually producing more fusile fuel than it consumed. Comparing said trajectories with those obtained from the formalism developed here it is apparent that they are quite sensitive to the quantities G_{10} and U_1. Therefore it must be cautioned that these values should be known quite accurately before applying this formalism to a practical case.

3.4 Concluding Remarks

It seems apparent that, in the analysis of fusion-fission symbiotic systems, the conventional practice of using a simple exponential nuclear fuel trajectory imposed by Eq. (3.0.1) can lead to overly optimistic results. This is even more true when dealing with isotopes

possessing shorter half-lives such as Tritium. Here a physically more justifiable approach has been taken to describe the fuel trajectories. This formalism seems to possess sufficient generality to be applied to a large set of possible fusion-fission systems if the forementioned sensitivities are taken into account.

APPENDIX

A DISCUSSION OF DOUBLING TIMES OF FUEL BREEDING SYSTEMS

In the description of a fuel breeding system, the most oft-quoted figure of merit is the fuel doubling time. As the name suggests this is the time required to produce enough fuel to start up a second identical reactor. There are basically two different doubling times which are based on differing assumptions.

The first doubling time, the linear doubling time, is based on the assumption that the fuel produced is proportional to the reactor power, i.e.

$$\frac{dN}{dt} = k\, P_o; \quad P_o = \text{power} \tag{A1.1}$$

If the reactor power, Po, is constant, and the initial amount of fuel is N_o, then the solution of (A1.1) is

$$N(t) = N_o + k\, P_o\, t \tag{A1.2}$$

which yields the linear doubling time

$$\tau_L = \frac{N_o}{k\, P_o} \tag{A1.3}$$

However, the assumption is sometimes made that the fuel be instantaneously "re-invested" to produce more power, this meaning power, P, is increasing with time leading to:

$$\frac{dN}{dt} = k\, P(t) \tag{A1.4}$$

Now, if the amount of power extracted from a given mass of fuel is constant then.

$$\frac{dN}{dt} = k\ \beta\ N \tag{A1.5}$$

where

$$\beta = \frac{P_o}{N_o}$$

The solution of (A1.3) becomes,

$$N(t) = N_o\ e^{k\beta t} \tag{A1.6}$$

yielding the exponential doubling time;

$$\tau_e = \frac{\log 2}{k\beta}$$

$$= \frac{\log 2}{k}\ \frac{N_o}{P_o}$$

$$= \tau_L \log 2 \tag{A1.7}$$

An exponentially increasing inventory implies the bred fuel is instantaneously reinvested and that this reinvestment is into an increasing number of reactors or a reactor increasing in size. This in turn implies the underlying assumptions are valid for a large number of reactors where continuous growth would be an adequate approximation. Clearly, for the first few reactors in an expanding system, as well as for a mixed reactor economy, this approximation is unwarranted.

REFERENCES

1. B.R. Leonard, Jr., "A Review of Fusion Fission Concepts", Nucl. Tech., 20, 1973, p. 161.

2. K.R. Schulz et al, "Prelimary Evaluation of a U-233 Fusion Fission Power System Without Reprocessing", Proc. of the Second Fusion-Fission Energy Systems Review Meeting, CONF-771155, Vol. 1, p. 187, Nov. 2, 1977.

3. A.G. Cook, "The Feasibility of U-233 Breeding in D-T Fusion Devices", M.Sc. Thesis, Massachusetts Institute of Technology, May 1976.

4. B.R. Leonard Jr., "Fissile Fuel Breeding and Hybrid Blanket Power Production", TANSAO 27, 1977, p. 339.

5. D.L. Jassby, "Fusion-Supported Decentralized Nuclear Energy System", Princeton Plasma Physics Laboratory Report PPPL-TM-316, 1978.

6. A.A. Harms and C.W. Gordon, "Fissile Fuel Breeding Potential with Paired Fusion-Fission Reactors", Annals Nuclear Energy, 3, 1976, 411.

7. P. Fortescue, "The Fusion Breeder Concept", Annals Nuclear Energy, 2, 1975, 29.

8. A.A. Harms, "Heirarchical Systematics of Fusion-Fission Energy Systems", Nuclear Fusion, 15, 1975, 939.

9. W.C. Gough, "EPRI/Kurchatov Institute Joint Program on Fusion-Fission", TANSAO 27, 1977, 340.

10. L.M. Lidsky, "Fission-Fusion Symbiosis: General Considerations and a Specific Example", Proc. Conf. Nuclear Fusion Reactors, Culham Laboratory, U.K., 1969.

11. H.W. Bonin et al., "The Importance of Protactinium in a Thorium-Fuelled CANDU Reactor", TANSAO 30, 1978, 717.

12. M.S. Milgram, "Some Physics Problems in the Design of Thorium-Fuelled CANDU Reactors", AECL Report, AECL-5561, August 1976.

13. V.L. Blinkin and V.M. Novikov, "Symbiotic System of a Fusion and a Fission Reactor with Very Simple Fuel Reprocessing", Nuclear Fusion, 18, 1978, p. 7.

14. W.B. Lewis, "World Prospects for the Development and use of Atomic Power", AECL Report No. Dr. 1, Mar. 1947.

15. P.R. Kasten et al., "The Thorium Fuel Cycle", TANSAO 28, 1978, p. 336.

16. P.R. Kasten et al., "The Thorium Fuel Cycle - A Nuclear Strategy and Fuel Recycle Technology", TANSAO, 29, 1978, 277.

17. P. Grand and H.J. Kouts, "Conceptual Design and Economic Analysis of a Light Water Reactor Fuel Regenerator", Brookhaven National Laboratory Report BNL-50838, May 15, 1978.

18. M.M. El-Wakil, "Nuclear Energy Conversion", International, p. 330, 1971.

19. J. Veeder, "Thorium Fuel Cycles in CANDU", TANSAO 29, 1978, 267.

20. A.A. Harms and M. Heindler, "Fissile Fuel Doubling Time Characteristics for Reactor Life-time Logistics", Nuc. Sci. Eng., 66, 1978.

BIBLIOGRAPHY

The following references, although not specifically used in this thesis contain useful information with regards to the Thorium Fuel cycle.

Cameron, D.J., A Review of the Potential for Actinide Redistribution in CANDU Thorium Cycle Fuels, AECL Report AECL-5962, Feb. 1978.

Duret, M.F. and Hatton, H., Some Thorium Fuel Cycle Strategies, AECL Report AECL-6414, Feb. 1979.

Milgram, M.S., Potential of Axial Fuel Management Strategies in Thorium-Fuelled CANDU'S, AECL Report AECL-6182, June 1978.